

5. EXPLANATORY NOTES¹

Shipboard Scientific Party²

INTRODUCTION

In this chapter we have assembled information that will help the reader understand the basis for our preliminary conclusions and also help the interested investigator select samples for further analysis. This information concerns only shipboard operations and analyses described in the site reports in this volume, *Initial Reports*. Methods used by various investigators for shore-based analysis of Leg 141 data will be detailed in the individual scientific contributions published in the *Scientific Results* volume.

AUTHORSHIP OF SITE CHAPTERS

The separate sections of the site chapters were written by the following shipboard scientists (authors are listed in alphabetical order, no seniority is necessarily implied):

Site Summary: Behrmann, Lewis

Background and Objectives: Behrmann, Lewis

Operations: Huey, Musgrave

Lithostratigraphy and Igneous Petrology: Forsythe, Kurnosov, Marsaglia, Strand, Vega, Vergara

Biostratigraphy: Boden, Müller (shore-based), Spiegler, Takahashi

Paleomagnetism: Collombat, Didenko, Musgrave

Structural Geology: Lindsley-Griffin, Osozawa, Prior

Organic Geochemistry: Didyk, Waseda

Inorganic Geochemistry: Froelich, Torres

Physical Properties: Brown, Scholl

WSTP and ADARA Temperature Measurements: Brown

Wireline Measurements: Bangs, Golovchenko, Sawyer

Summary and Conclusions: Behrmann, Lewis

Following the text of each site chapter are summary core descriptions ("barrel sheets" and igneous rock visual core descriptions) and photographs of each core.

SURVEY AND DRILLING DATA

Geophysical survey data collected during Leg 141 fall into two categories: (1) magnetic and bathymetric data acquired during transits from Panama to Valparaiso, from Valparaiso to Site 859, and from Site 863 to Valparaiso, and (2) data collected between sites. These data are discussed in the Underway Geophysics section (this volume), along with a brief description of all geophysical instrumentation and acquisition systems used, and a summary listing of Leg 141 navigation. The survey data used for final site selection, including data collected during site surveys prior to Leg 141 are presented in the Seismic Stratigraphy section of the individual site chapters (this volume). During the Leg 141 *JOIDES Resolution* surveys, single-channel seismic, and 3.5- and

12-kHz echo sounder data were recorded across the planned drilling sites to aid site confirmation prior to dropping the beacon.

The single-channel seismic profiling system used two 80-in³ water guns as the energy source and a Teledyne streamer with a 100-m-long active section. These data were recorded digitally on tape using a Masscomp 561 super minicomputer, and were also displayed in real time in analog format on two Raytheon recorders using a variety of filter settings (commonly 30–140 Hz) and two different scales (commonly 1- and 2-s sweeps and 50 traces/in.).

Bathymetric data collected using the 3.5- and 12-kHz Precision Depth Recorder (PDR) system were displayed on two Raytheon recorders. The depths were calculated on the basis of an assumed 1463-m/s sound velocity in water. The water depth (in meters) at each site was corrected for (1) the variation in sound velocity with depth using Matthews' (1939) tables, and (2) the depth of the transducer pod (6.8 m) below sea level. In addition, depths referred to the drilling-platform level are corrected for the height of the rig floor above the water line, which gradually increased from 11.07 to 11.65 m throughout the cruise (see Fig. 1).

Magnetic data were collected using a Geometrics 801 proton precession magnetometer, displayed on a strip-chart recorder and recorded on magnetic tape for later processing.

Drilling Characteristics

Because water circulation downhole is open, cuttings are lost onto the seafloor and cannot be examined. Information concerning sedimentary stratification in uncored or unrecovered intervals may be inferred from seismic data, wireline-logging results, and from an examination of the behavior of the drill string as observed and recorded on the drilling platform. Typically, the harder a layer, the slower and more difficult it is to penetrate. A number of other factors may determine the rate of penetration, so it is not always possible to relate the drilling time directly to the hardness of the layers. Bit weight and revolutions per minute, recorded on the drilling recorder, also influence the penetration rate.

Drilling Deformation

When cores are split, many show signs of significant sediment disturbance, including the concave-downward appearance of originally horizontal bands, haphazard mixing of lumps of different lithologies (mainly at the tops of cores), and the near-fluid state of some sediments recovered from tens to hundreds of meters below the seafloor. Core deformation probably occurs during cutting, retrieval (with accompanying changes in pressure and temperature), and core handling on deck.

SHIPBOARD SCIENTIFIC PROCEDURES

Numbering of Sites, Holes, Cores, and Samples

Drilling sites are numbered consecutively from the first site drilled by the *Glomar Challenger* in 1968. A site number refers to one or more holes drilled while the ship was positioned over one acoustic beacon. Multiple holes may be drilled at a single site by pulling the drill pipe above the seafloor (out of the hole),

¹ Behrmann, J.H., Lewis, S.D., Musgrave, R.J., et al., 1992. *Proc. ODP, Init. Repts.*, 141: College Station, TX (Ocean Drilling Program).

² Shipboard Scientific Party is as given in the list of participants preceding the contents.

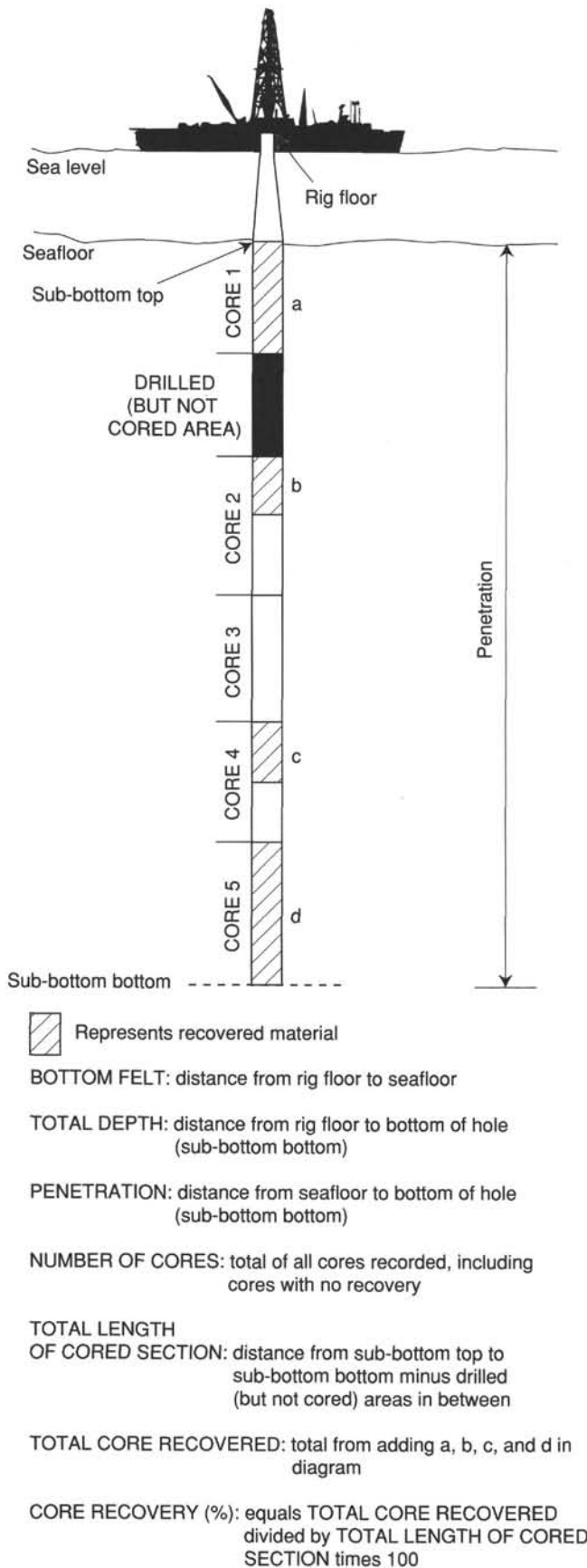


Figure 1. Diagram illustrating terms used in the discussion of coring operations and core recovery.

moving the ship some distance from the previous hole, and then drilling another hole. In some cases, the ship may return to a previously occupied site to drill additional holes.

For all ODP drill sites, a letter suffix distinguishes each hole drilled at the same site. For example, the first hole drilled is assigned the site number modified by the suffix A, the second hole takes the site number and suffix B, and so forth. Note that this procedure differs slightly from that used by DSDP (Sites 1 through 624), but prevents ambiguity between site- and hole-number designations. It is important to distinguish among holes drilled at a site, because recovered sediments or rocks from equivalent depths in different holes do not necessarily come from equivalent positions in the stratigraphic column.

The cored interval is measured in meters below seafloor (mbsf); sub-bottom depths are determined by subtracting the drill-pipe measurement (DPM) water depth (the length of pipe from the rig floor to the seafloor) from the total DPM (from the rig floor to the bottom of the hole; see Fig. 1). Note that although the echo-sounding data (from the precision depth recorders) are used to locate the site, they are not used as a basis for any further measurements.

The depth interval assigned to an individual core begins with the depth below the seafloor at which the coring operation began, and extends to the depth that the coring operation ended for that core (see Fig. 1). For rotary coring (RCB and XCB), each coring interval is equal to the length of the joint of drill pipe added for that interval (though a shorter core may be attempted in special instances). The drill pipe in use varies from about 9.4 to 9.8 m. The pipe is measured as it is added to the drill string, and the cored interval is recorded as the length of the pipe joint to the nearest 0.1 m. For hydraulic piston coring (APC) operations, the drill string is advanced 9.5 m, the maximum length of the piston stroke.

Coring intervals may be shorter and may not necessarily be adjacent if separated by drilled intervals. In soft sediments, the drill string can be "washed ahead" with the core barrel in place, without recovering sediments. This is achieved by pumping water down the pipe at high pressure to wash the sediment out of the way of the bit and up the annulus between the drill pipe and the wall of the hole. If thin, hard, rock layers are present, then it is possible to get "spotty" sampling of these resistant layers within the washed interval, and thus to have a cored interval greater than 9.5 m. In drilling hard rock, a center bit may replace the core barrel if it is necessary to drill without core recovery.

Cores taken from a hole are numbered serially from the top of the hole downward. Core numbers and their associated cored intervals in meters below seafloor usually are unique in a given hole; however, this may not be true if an interval must be cored twice, because of caving of cuttings or other hole problems. Maximum full recovery for a single core is 9.5 m of rock or sediment contained in a plastic liner (6.6-cm internal diameter) plus about 0.2 m (without a plastic liner) in the core catcher (Fig. 2). The core catcher is a device at the bottom of the core barrel that prevents the core from sliding out when the barrel is being retrieved from the hole. For sediments, the core-catcher sample is extruded into a short piece of plastic liner and is treated as a separate section below the last core section. For hard rocks, material recovered in the core catcher is included at the bottom of the last section. In certain situations (e.g., when coring gas-charged sediments that expand while being brought on deck) recovery may exceed the 9.5-m maximum.

A recovered sedimentary core is divided into 1.5-m sections that are numbered serially from the top (Fig. 2). When full recovery is obtained, the sections are numbered from 1 through 7, with the last section possibly being shorter than 1.5 m (rarely, an unusually long core may require more than seven sections). When less than full recovery is obtained, there will be as many sections

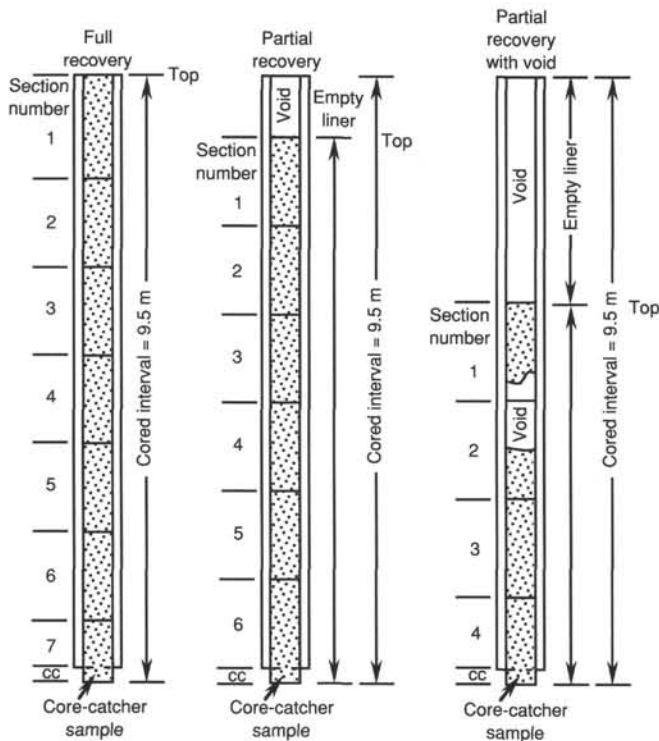


Figure 2. Diagram showing procedure used in cutting and labeling core sections.

as needed to accommodate the length of the core recovered; for example, 4 m of core would be divided into two 1.5-m sections and one 1-m section. If cores are fragmented (recovery less than 100%), sections are numbered serially and intervening sections are noted as void, whether shipboard scientists believe that the fragments were contiguous in situ or not. In rare cases a section less than 1.5 m may be cut to preserve features of interest (e.g., lithologic contacts).

By convention, during the core description, material recovered from the core catcher of a sedimentary core is placed in a separate section labeled core catcher (CC) below the last section recovered in the liner. The core catcher is placed at the top of the cored interval in cases where material is only recovered in the core catcher. However, information supplied by the drillers or by other sources may allow for more precise interpretation as to the correct position of core-catcher material within an incompletely recovered cored interval.

Igneous rock cores are also cut into 1.5-m-sections that are numbered serially; individual pieces of rock are then each assigned a number. Fragments of a single piece are assigned a single number, and individual fragments are identified alphabetically. The core-catcher sample is placed at the bottom of the last section and is treated as part of the last section, rather than separately. Scientists completing visual core descriptions describe each lithologic unit, noting core and section boundaries only as physical reference points.

When, as is usually the case, the recovered core is shorter than the cored interval, the top of the core is equated with the top of the cored interval by convention, to achieve consistency in handling analytical data derived from the cores. Samples removed from the cores are designated by distance measured in centimeters from the top of the section to the top and bottom of each sample removed from that section. In curated hard-rock sections, sturdy plastic spacers are placed between pieces that did not fit together,

to protect them from damage in transit and in storage; therefore, the centimeter interval noted for a hard-rock sample has no direct relationship to that sample's depth within the cored interval, but is only a physical reference to the location of the sample within the curated core.

A full identification number for a sample consists of the following information: leg, site, hole, core number, core type, section number, piece number (for hard rock), and interval in centimeters measured from the top of section. For example, a sample identification of "141-859A-5H-1, 10–12 cm" would be interpreted as representing a sample removed from the interval between 10 and 12 cm below the top of Section 1, Core 5 (H designates that this core was taken during hydraulic piston coring) of Hole 859A during Leg 141.

All ODP core and sample identifiers indicate core type. The following abbreviations are used: R = rotary core barrel (RCB); H = hydraulic piston core (HPC; also referred to as APC, or advanced hydraulic piston core); P = pressure core sampler (PCS); X = extended core barrel (XCB); B = drill-bit recovery; C = center-bit recovery; I = in situ water sample; N = motor-driven core barrel (MDCB); S = side-wall sample; W = wash-core recovery; and M = miscellaneous material. APC, XCB, RCB, PCS, and MDCB cores were cut on Leg 141.

Core Handling

Sediments

As soon as a core is retrieved on deck, a sample is taken from the core catcher and given to the paleontological laboratory for an initial age assessment. The core is then placed on the long horizontal rack, and gas samples may be taken by piercing the core liner and withdrawing gas into a vacuum-tube ("Vacutainer"). Voids within the core are sought as sites for gas sampling. While collection of gases both for storage for shore-based study and for immediate analysis as part of the shipboard safety and pollution-prevention program is standard ODP practice, an additional emphasis on gas collection and analysis was placed by the gas hydrate studies conducted on Leg 141. Next, the core is marked into section lengths, each section is labeled, and the core is cut into sections. Interstitial-water (IW) whole-round samples are then taken as a matter of ODP policy; other whole-round samples for organic geochemistry may also be taken at this stage (as they were on Leg 141) if they have been specifically requested. In addition, some headspace gas samples are scraped from the ends of cut sections on the catwalk, and sealed in glass vials for light hydrocarbon analysis. Each section is then sealed at the top and bottom by gluing on color-coded plastic caps, blue to identify the top of a section and clear for the bottom. A yellow cap is placed on the section ends from which a whole-round sample has been removed, and the sample code (e.g., IW) is written on the yellow cap. The caps are usually attached to the liner by coating the end liner and the inside rim of the cap with acetone, and the caps are then taped to the liners.

The cores then are carried into the laboratory, where the sections are again labeled, using an engraver to permanently mark the full designation of the section. The length of the core in each section and the core-catcher sample are measured to the nearest centimeter; this information is logged into the shipboard CORE-LOG database program.

Sections from APC and XCB cores are normally run through the Multisensor Track (MST) before splitting. The MST includes the GRAPE (gamma-ray attenuation porosity evaluator) and P-wave logger devices, which measure bulk density, porosity, and sonic velocity, and also includes a meter that determines the volume magnetic susceptibility. At this point, whole-round samples for physical properties (PP) and structural analysis are taken.

In well-lithified sedimentary cores, the core liner is split and the top half removed so that the whole-round core can be observed before choosing the samples. Relatively soft sedimentary cores are equilibrated to room temperature (approximately 3 hr) and thermal conductivity measurements are performed on them.

Cores of unlithified and moderately lithified material are split lengthwise into working and archive halves. The softer cores are split with a wire or saw, depending on the degree of induration. Harder cores are split with a band saw or diamond saw. The wire-cut cores are split from the bottom to top, so investigators should be aware that older material could have been transported up the core on the split face of each section.

The working half of the core is sampled for both shipboard and shore-based laboratory studies. Each extracted sample is logged into the sampling computer database program by the position of the sample and the name of the investigator receiving the sample. Records of all removed samples are kept by the curator at ODP. The extracted samples are sealed in plastic vials or bags and labeled. Samples are routinely taken for shipboard physical property analysis. These samples are subsequently used for calcium carbonate (coulometric analysis) and organic carbon (CNS elemental analyzer) and the data are reported in the site chapters.

The archive-half is described visually. Smear slides are made from samples taken from the archive-half and are supplemented by thin sections taken from the working half. Most archive sections are run through the cryogenic magnetometer. The archive-half is then photographed with both black-and-white and color film, a whole core at a time. Close-up photographs (black-and-white) are taken of particular features for illustrations in the summary of each site, as requested by individual scientists.

Both halves of the core are then put into labeled plastic tubes, sealed, and transferred to cold-storage space aboard the drilling vessel. At the end of the leg, the cores are transferred from the ship in refrigerated airfreight containers to cold storage at the Gulf Coast Repository at the Ocean Drilling Program, Texas A&M University, College Station, Texas.

Igneous and Metamorphic Rocks

Igneous and metamorphic rock cores are handled differently from sedimentary cores. Once on deck, the core catcher is placed at the bottom of the core liner and total core recovery is calculated by shunting the rock pieces together and measuring to the nearest centimeter; this information is logged into the shipboard core-log database program. The core is then cut into 1.5-m-long sections and transferred into the lab.

The contents of each section are transferred into 1.5-m-long sections of split core liner, where the bottom of oriented pieces (i.e., pieces that clearly could not have rotated top to bottom about a horizontal axis in the liner) are marked with a red wax pencil. This is to ensure that orientation is not lost during the splitting and labeling process. The core is then split into archive and working halves. A plastic spacer is used to separate individual pieces and/or reconstructed groups of pieces in the core liner. These spacers may represent a substantial interval of no recovery. Each piece is numbered sequentially from the top of each section, beginning with number 1; reconstructed groups of pieces are assigned the same number, but are lettered consecutively. Pieces are labeled only on external surfaces. If the piece is oriented, an arrow is added to the label pointing to the top of the section.

The working half of the hard-rock core is then sampled for preliminary shipboard laboratory studies (typically paleomagnetism, X-ray fluorescence, and thin-section examination). Personal sampling is conducted at a time when all hard-rock investigators can sample together as a group. Records of all samples are kept by the curator at ODP.

The archive-half is described visually, then photographed with both black-and-white and color film, one core at a time. Both halves of the core are then shrink-wrapped in plastic to prevent rock pieces from vibrating out of sequence during transit, put into labeled plastic tubes, sealed, and transferred to cold-storage space aboard the drilling vessel. As with the other Leg 141 cores, they are housed in the Gulf Coast Repository.

Fluids

In addition to the routine recovery of gas and liquid samples from sediment cores brought on deck, techniques have been developed for the recovery of fluids at conditions near to those applying in situ down the drill hole. The pressure core sampler (PCS) maintains down-hole hydrostatic pressures up to approximately 70 MPa (10,000 lb/in.²) while recovering a core sample with a nominal diameter of 42 mm and a length of 0.86 m. Although direct sampling of the pressured core is not yet possible, fluid and gas samples can be recovered. The WSTP (water-sampling temperature probe) extracts interstitial water from sediments at the bottom of the hole after being lowered down the drill pipe on the sandline. Its filter probe extends more than 1 m beyond the end of the drill bit.

VISUAL CORE DESCRIPTION

Core Description Forms and the "VCD" Program

The core description forms (Fig. 3), or "barrel sheets," summarize the data obtained during shipboard analysis of each sediment core. On Leg 141 these were generated using the ODP in-house Macintosh application "VCD" (edition 1.0.Op1, customized for this leg). The following discussion explains the ODP conventions used in compiling each part of the core description forms, the use of "VCD" to generate these forms, and the exceptions to these procedures adopted by the Leg 141 shipboard party.

Shipboard sedimentologists were responsible for visual core logging, smear-slide analyses, and thin-section descriptions of sedimentary and volcanoclastic material. Core descriptions were initially recorded by hand on a section-by-section basis on standard ODP Visual Core Description forms (VCD forms, not to be confused with the "VCD" Macintosh application). Use of these forms is now considered optional by ODP, and on some recent legs visual description was carried out directly at the core-by-core level using the VCD application. On Leg 141, however, we considered it desirable to preserve fine-detail observations that are lost at the core-by-core "barrel sheet" level. Structural geologists also recorded structures on VCD forms of their own design. Copies of the Visual Core Description forms are available from ODP on request.

Hand-drawn "barrel sheets," used by ODP up through Leg 135, included columns for information on biostratigraphic zonation, geochemistry (CaCO₃, C_{org}, XRF), paleomagnetism, and physical properties (wet-bulk density and porosity). Much of this information is redundant at the core-by-core level. Core description forms generated directly by the VCD Macintosh application comprise a condensed version of the information normally recorded on the section-by-section Visual Core Description sheets, supplemented only by a column indicating age. However, the VCD application offers an alternate representation of the core description forms as a PICT file, allowing their manipulation by Macintosh graphics applications. By this means it is possible to attach columns with additional graphics or text information (e.g., magnetostratigraphy, chemical data, GRAPE data, magnetic susceptibility) as desired. Customization of the VCD application allowed the addition of sedimentary structures, graphic lithologies, and other features specific to this leg.

SITE 860 HOLE B CORE 58X				CORED 492.8 - 502.4 mbsf				
Meter	Graphic Lith.	Section	Age	Structure	Disturb	Sample	Color	Description
0.5		1	Lower Pliocene	↑ F ⋈		S	5Y 3/2 To 5Y 4/1	SANDY SILTY CLAYSTONE TO SILTY CLAYSTONE Major Lithology: The core consists of olive gray (5Y 3/2 and 5Y 4/1), poorly sorted SANDY SILTY CLAYSTONE and SILTY CLAYSTONE and shows four 80-150 cm thick fining-upward sequences. In Section 1 the lower 5 cm of one distinct sequence is inverse graded and there occurs a gradual change from sandy silty claystone to silty claystone in the interval 65 to 70 cm. General Description: Toward the base of each fining-upward sequence there are clast concentrations, isolated lithic clasts and some shell fragments and the sediments have a matrix-supported texture. The clasts consist of calcareous sedimentary fragments, pyrite concretions, and blackish volcanic clasts containing pyrite. Maximum clast size is 1.8 cm. These sediments contain a minor proportion (up to 10%) of micritic carbonate. Dark seams are found throughout the core.
1.0								
1.5								
2.0								
2.5								
3.0								
3.5								
4.0								
4.5								
5.0								
	CC			↑ F ⋈		I W S S		
				↑ F ⋈		M		

Figure 3. Core description form ("barrel sheet") used for sediments and sedimentary rocks.

For each hole a Master Chart was prepared (Fig. 4), which indicated recovery, summarized the lithology, and charted a variety of data against sub-bottom depth (biostratigraphic zones, magnetic polarity and magnetochrons, structural geology, fluid chemistry, physical properties, logging characteristics, paleo-water temperatures, and paleodepths). The Master Charts supplement the information contained on the core description forms, at a further condensed scale.

Core Designation

Cores are designated using leg, site, hole, core number, and core type as discussed in a preceding section (see Numbering of Sites, Holes, Cores, and Samples section, this chapter). The cored interval is specified in terms of meters below sea level (mbsl) and meters below seafloor (mbsf). On the basis of drill-pipe measurements (dpm), reported by the SEDCO coring technician and the ODP operations superintendent, depths are corrected for the height of the rig floor dual elevator stool above sea level to give true water depth and correct mbsl.

Graphic Lithology Column

The lithology of the material recovered is represented on the core description forms by up to three symbols in the column titled "Graphic Lithology" (Fig. 5). Where an interval of sediment or sedimentary rock is a homogenous mixture, the constituent categories are separated by a solid vertical line, with each category represented by its own symbol. Constituents accounting for <10% of the sediment in a given lithology (or others remaining after the representation of the three most abundant lithologies) are not shown in the graphic lithology column but are listed in the "Description" section of the core description form. In an interval comprising two or more sediment lithologies that have quite

different compositions, such as in thin-bedded and highly variegated sediments, the average relative abundances of the lithologic constituents are represented graphically by dashed lines that vertically divide the interval into appropriate fractions, as described above. The graphic lithology column shows only the composition of layers or intervals exceeding 20 cm in thickness. This information is available upon request from ODP.

Age Column

The chronostratigraphic unit, as recognized on the basis of paleontological and paleomagnetic criteria, is shown in the "Age" column on the core description forms. Boundaries between assigned ages are indicated as follows:

1. Sharp boundary: straight line;
2. Unconformity or hiatus: line with + signs above it;
3. Uncertain: line with question marks.

Sedimentary Structures

In sediment cores, natural structures and structures created by the coring process can be difficult to distinguish. Natural structures observed are indicated in the "Structure" column of the core description forms. The column is divided into three vertical areas for symbols (Fig. 6).

Sediment Disturbance

Sediment disturbance resulting from the coring process is illustrated in the "Disturbance" column on the core description forms (using symbols in Fig. 6). Blank regions indicate a lack of drilling disturbance. The degree of drilling disturbance is described for soft and firm sediments using the following categories:

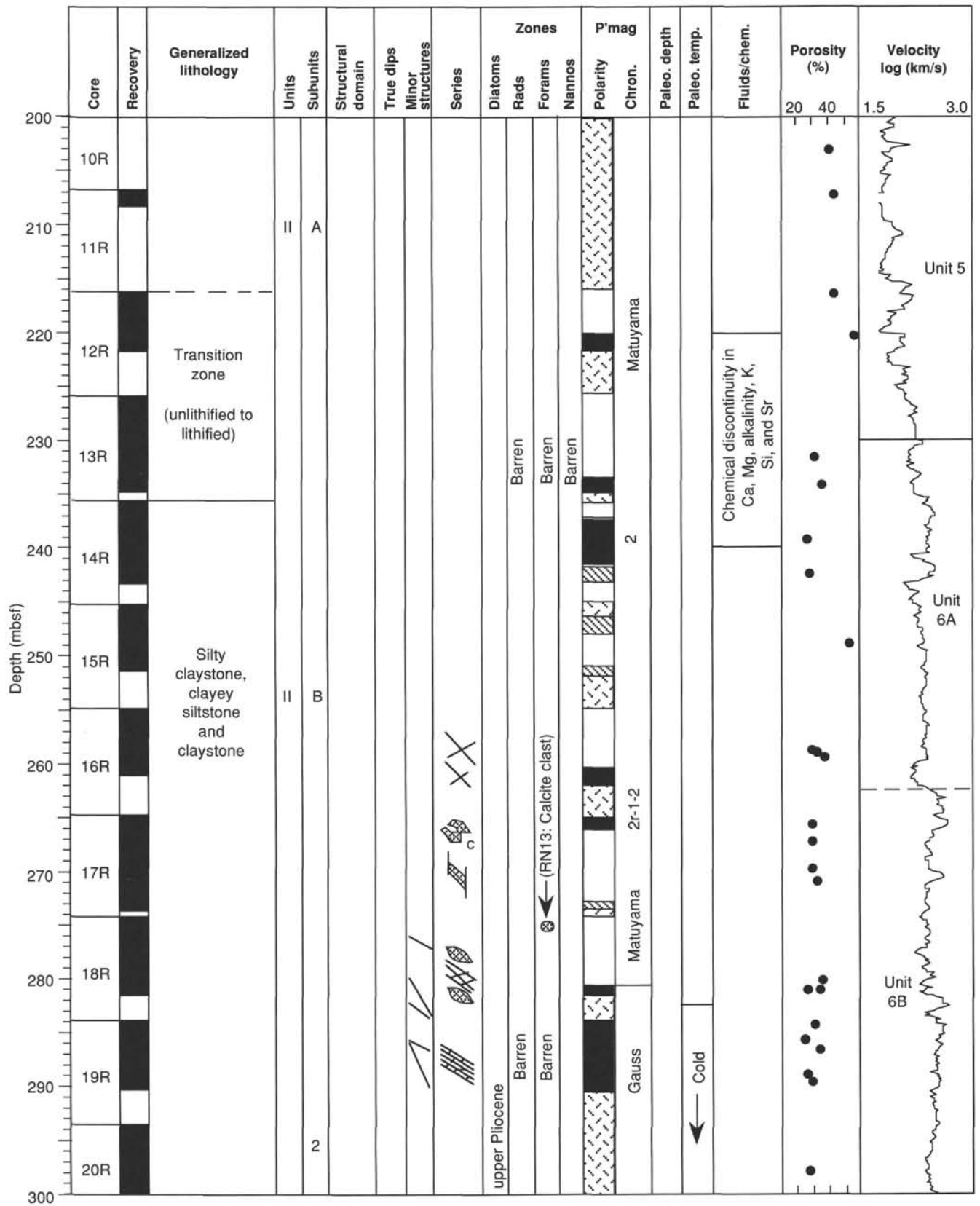


Figure 4. Example of a hole Master Column.

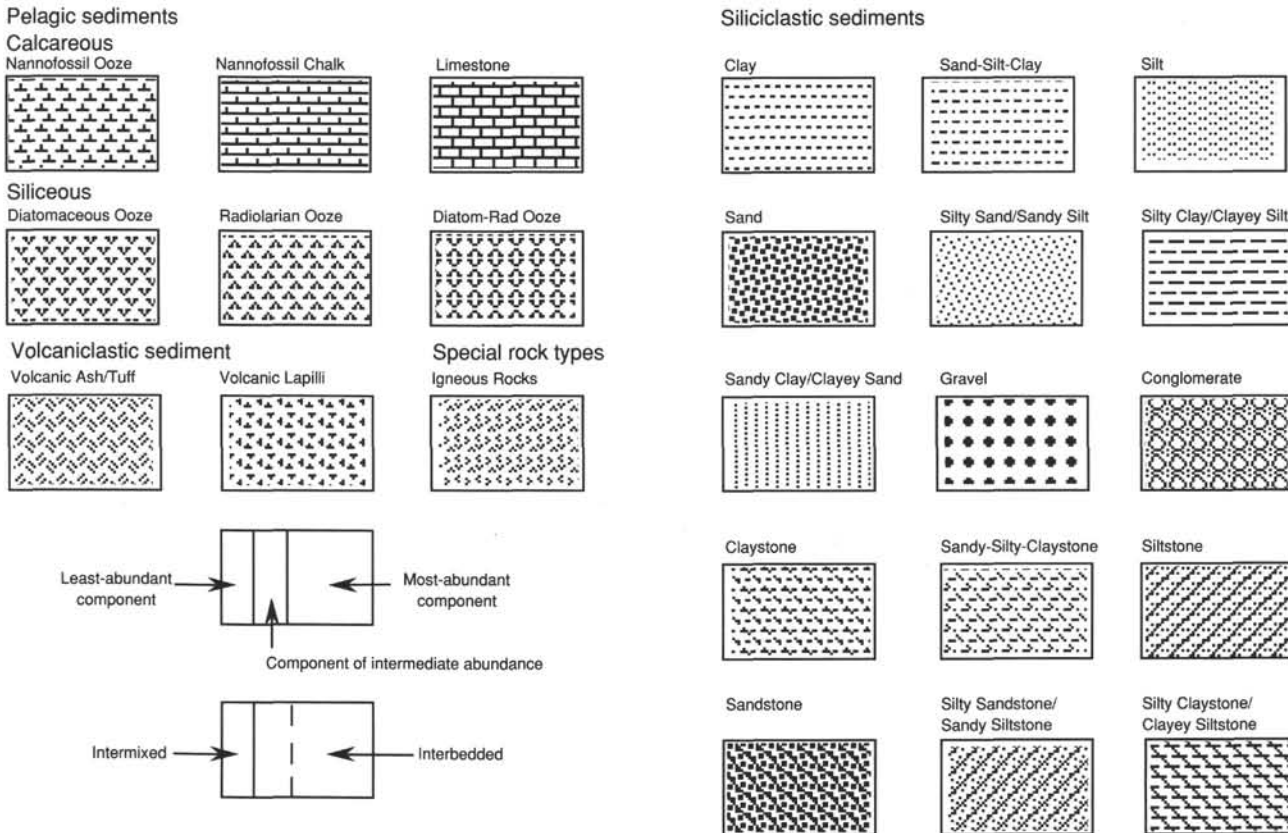


Figure 5. Key to symbols used in the "graphic lithology" column on the core description form shown in Figure 3.

1. Slightly deformed: bedding contacts are slightly bent.
2. Moderately deformed: bedding contacts have undergone extreme bowing.
3. Highly deformed: bedding is completely disturbed, sometimes showing symmetrical diapir-like or flow structures.
4. Soupy: intervals are water saturated and have lost most to all aspects of original bedding.

The degree of fracturing in indurated sediments and igneous rocks is described using the following categories:

1. Slightly fractured: core pieces are in place and contain little drilling slurry or breccia;
2. Moderately fragmented: core pieces are in place or partly displaced, but original orientation is preserved or recognizable (drilling slurry may surround fragments);
3. Highly fragmented: pieces are from the interval cored and probably in correct stratigraphic sequence (although they may not represent the entire section), but original orientation is completely lost;
4. Drilling breccia: core pieces have lost their original orientation and stratigraphic position and may be mixed with drilling slurry.

Color

The hue and chroma attributes of color were determined by comparison with Munsell soil-color charts (Munsell Soil Color Charts, 1971). This was done as soon as possible after the cores were split because redox-associated color changes may occur when deep-sea sediments are exposed to the atmosphere. Infor-

mation on core colors is given in the "Color" column on the core description forms.

Samples

The position of samples taken from each core for shipboard analysis is indicated in the "Samples" column on the core description form, as follows:

- S: smear slide
- T: thin section
- M: micropaleontology sample
- I: interstitial water sample
- W: other whole-round samples

Smear-Slide Summary

A figure summarizing data from smear slides appears in each site chapter and a table summarizing data from smear slides and thin sections appears in the Appendix (this volume). The table includes information on the sample location, whether the sample represents a dominant ("D") or a minor ("M") lithology in the core, and the estimated percentages of sand, silt, and clay, together with all identified components.

Lithologic Description—Text

The lithologic description that appears on each core description form consists of three parts: (1) a heading that lists all the major sediment lithologies (see Sedimentology section, this chapter) observed in the core; (2) a heading for minor lithologies, and (3) a more detailed description of these sediments, including features such as color, composition (determined from the analysis of smear slides), sedimentary structures, or other notable charac-

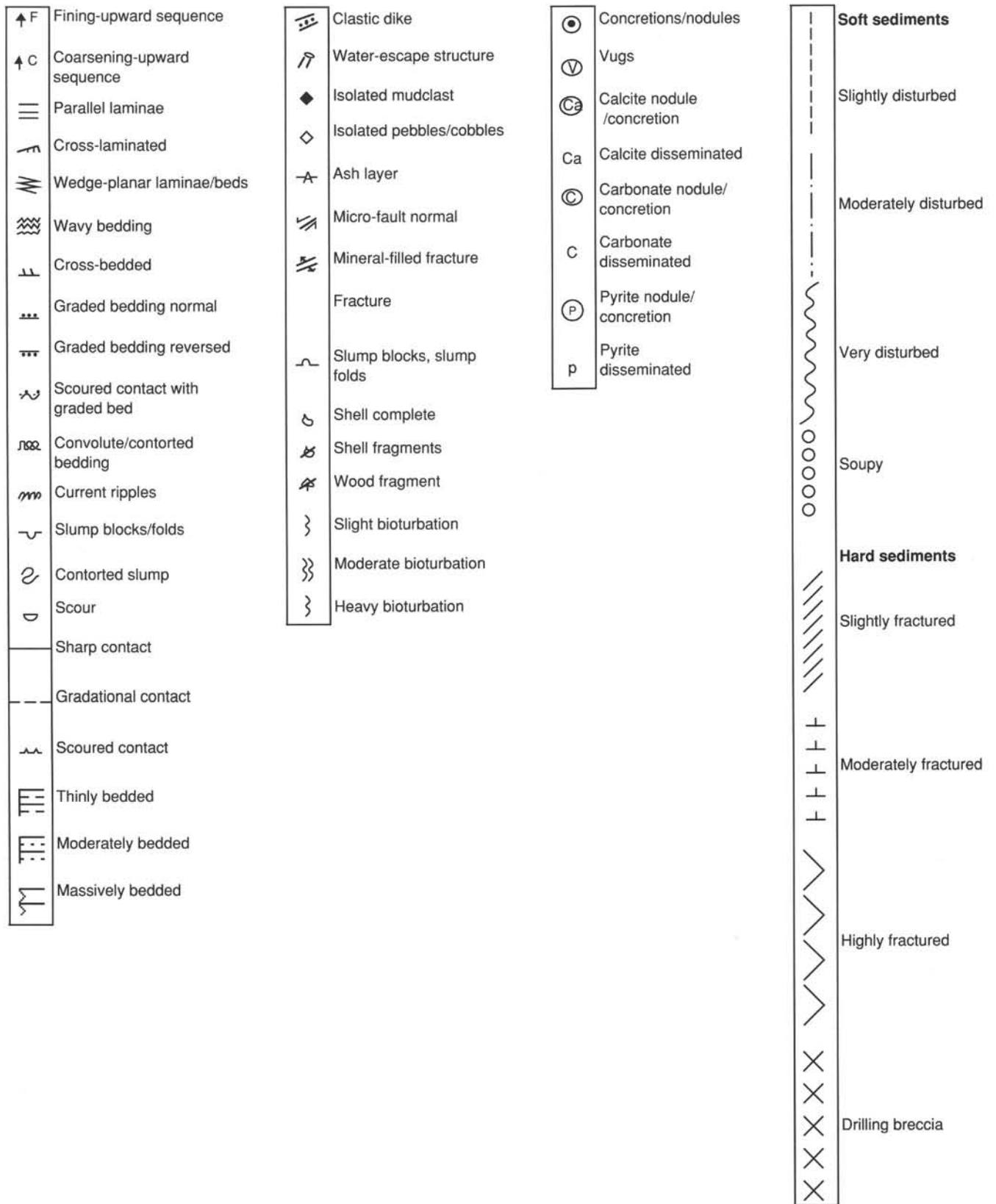


Figure 6. Symbols used for drilling disturbance and sedimentary structure on core description forms shown in Figure 3.

teristics. Descriptions and locations of thin, interbedded, or minor lithologies that cannot be depicted in the graphic lithology column are included in the text.

SEDIMENTOLOGY

Classification of Sediments and Sedimentary Rocks

Leg 141 used a modified version of the sediment classification scheme of the Ocean Drilling Program (Shipboard Scientific Party, 1990; Mazzullo et al., 1987) for granular sediment types (Fig. 7). Variations in the relative proportions of pelagic, siliciclastic, and pyroclastic grain types define four major classes of granular sediments; any neritic component (e.g., bioclasts and shallow-water benthic foraminifers) is minor. Pelagic grains are the skeletal remains of open-marine siliceous and calcareous microfauna and microflora (e.g., radiolarians, diatoms, planktonic foraminifers, nannofossils) and associated organisms. Siliciclastic grains are mineral and rock fragments derived from igneous (plutonic and volcanic), sedimentary, and metamorphic rocks. Volcaniclastic grains include those of pyroclastic (direct products of magma degassing or water/magma interaction) and epiclastic (detritus derived from erosion of volcanic rocks) origins.

A granular sediment is classified by designating a principal name and major and minor modifiers. The principal name of a granular sediment defines its granular-sediment class; the major and minor modifiers describe the texture, composition, and fabric (Fig. 7).

Principal Names

For siliciclastic sediment, the principal name describes the texture and is assigned according to the following guidelines:

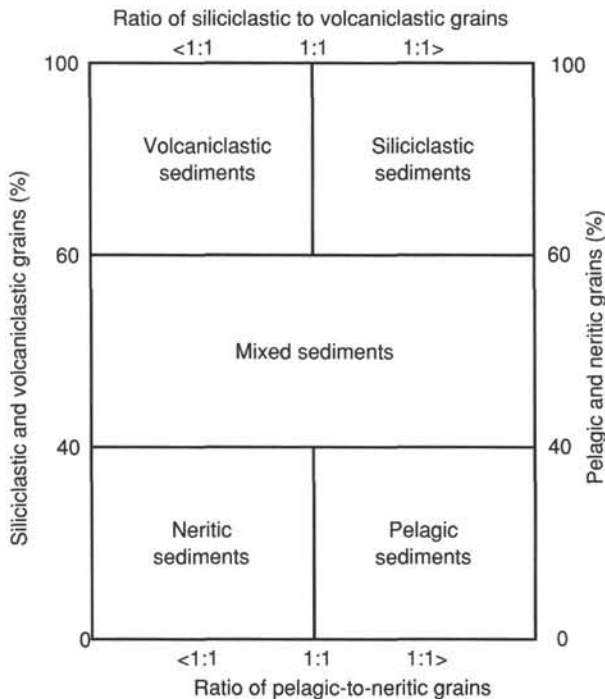


Figure 7. Diagram showing classes of granular sediment (modified from Mazzullo et al., 1987).

Millimeters	Micrometers	Phi (φ)	Wentworth size class	
4096		-12.0	Boulder	
256		-8.0	Cobble	
84		-6.0	Pebble	
4		-2.0	Granule	
2.00		-1.0	Very coarse sand	
1.00		0.0	Course sand	
1/2	0.50	500	1.0	Medium sand
1/4	0.25	250	2.0	Fine sand
1/8	0.125	125	3.0	Very fine sand
1/16	0.0625	63	4.0	Course silt
1/32	0.031	31	5.0	Medium silt
1/64	0.0156	15.6	6.0	Fine silt
1/128	0.0078	7.8	7.0	Very fine silt
1/256	0.0039	3.9	8.0	Clay
	0.00006	0.06	14.0	

Figure 8. Udden-Wentworth grain-size scale for siliciclastic sediments (Wentworth, 1922).

1. The Udden-Wentworth grain-size scale (Wentworth, 1922; Fig. 8) defines grain-size ranges and names of the textural groups (gravel, sand, silt, and clay) and subgroups (fine sand, coarse silt, etc.) that are used as the principal names of siliciclastic sediment.

2. Principal names are listed in order of increasing abundance when two or more textural groups or subgroups are present in a siliciclastic sediment (Shepard, 1954; Fig. 9). For simplicity, we have grouped intermediate mixtures of the three textural end members, sand, silt, and clay, into four categories (i.e., sandy clay/clayey sand, silty clay/clayey silt, silty sand/sandy silt, sandy silty clay).

3. The suffix -stone is affixed to the principal names sand, silt, and clay when the sediment is lithified. Conglomerate and breccia are used as principal names of lithified gravels with well-rounded and angular clasts, respectively.

Volcaniclastic sediments are subdivided into two groups, pyroclastic and epiclastic, with the principal name in each group describing

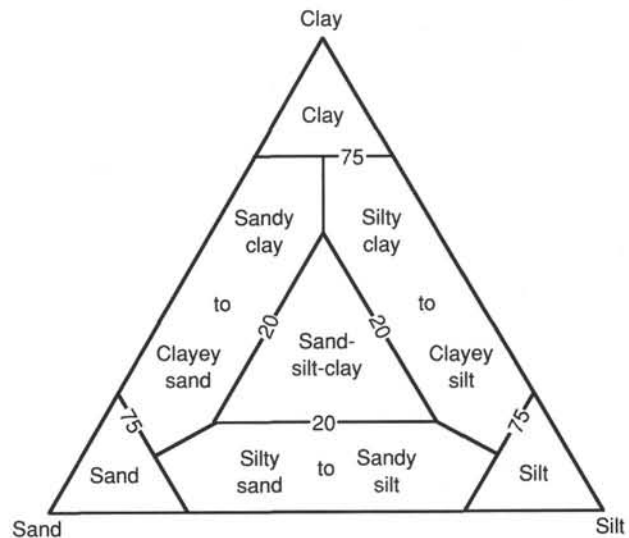


Figure 9. Ternary diagram showing principal names for siliciclastic sediments (modified from Shepard, 1954).

texture. The names and ranges of three textural groups for pyroclastic sediments/rocks (Fisher and Schmincke, 1984) are as follows:

1. Volcanic breccia: pyroclasts >64 mm in diameter;
2. Volcanic lapilli: pyroclasts between 2 and 64 mm in diameter; when lithified, use the name lapillistone;
3. Volcanic ash: pyroclasts <2 mm in diameter; when lithified, use the name tuff. For Leg 141, this group was subdivided into two classes by grain size: coarse ash/tuff, with grains between 1/16 and 2 mm in size, and fine ash/tuff, with grains <1/16 mm in size.

Epiclastic sediments, like siliciclastic sediments, are classified based on grain texture according to the Udden-Wentworth grain-size scale. The textural principal name is preceded by the modifier "volcaniclastic" (e.g., volcaniclastic conglomerate, volcaniclastic sand). Other rules apply as listed above for siliciclastic sediments.

For pelagic sediment, the principal name describes the composition and degree of consolidation using the following terms:

1. Ooze: unlithified calcareous and/or siliceous pelagic sediments;
2. Chalk: partially lithified pelagic sediment predominantly composed of calcareous pelagic grains;
3. Limestone: lithified pelagic sediment predominantly composed of calcareous pelagic grains; and
4. Radiolarite, diatomite, and spiculite: partially lithified pelagic sediment predominantly composed of siliceous radiolarians, diatoms, and sponge spicules, respectively.

Major and Minor Modifiers

The principal name of a granular sediment class is preceded by major modifiers and followed by minor modifiers (preceded by "with") that describe the lithology of the granular sediment in greater detail. Major and minor modifiers are used most commonly to describe composition and textures of grain types present in major (>25%) and minor (10%–25%) proportions and to describe grain fabric (e.g., matrix supported).

Composition of pelagic grains can be described with the major and minor modifiers diatom(-aceous), radiolarian, spicule(-ar), siliceous, nannofossil, foraminifer(-al), and calcareous. The terms siliceous and calcareous are used generally to describe sediments composed of siliceous or calcareous pelagic grains of mixed origins. Sediment fabric can be described by the major modifiers grain-supported or matrix-supported. Generally, fabric descriptors are applied only to gravels, conglomerates, and breccias.

The degree of consolidation is described using the following major modifiers: "unlithified" designates soft sediment that is readily deformable under the pressure of a finger, "partially lithified" designates firm sediment that is incompletely lithified, and "lithified" designates hard, cohesive sedimentary rock.

Grain shapes are described by the major modifiers rounded, subrounded, subangular, and angular. Sediment color is determined with the Munsell Chart, a standard color-comparator, and can be employed as a major modifier.

Mixed sediments are described using major and minor modifiers indicating composition and texture.

X-ray Diffraction Methods for Fine Fractions

The fine fraction of selected samples was analyzed on board using X-ray diffraction techniques. Sediments were put into suspension, and the fine fraction (less than 0.001 mm) was separated using a decantation method. The upper 5–7 cm of suspended material was removed after 24 hr, concentrated, and then used to prepare air-dried, oriented specimens on glass slides. X-ray diffraction patterns of these oriented specimens were produced using the shipboard Philips AD 3420 X-ray diffractometer (Cu K α

emission). After this initial analysis, each sample was then treated with ethylene glycol, reanalyzed, then heated at 550°C for 1 to 1.5 hr, and then analyzed again. Peaks were visually inspected and matched to standard reference peaks for various minerals (quartz, feldspar, hornblende, calcite, pyrite, and clay minerals, etc.). Semiquantitative analysis of the relative proportions of clay minerals in the fine fraction was made using a peak-height method outlined by Biscaye (1964): smectite (17Å)/illite (10Å)/chlorite + kaolinite (7Å) = 1/4/2.

BIOSTRATIGRAPHY

Chronological Framework

Three microfossil groups were examined on board for biostratigraphic purposes on Leg 141: diatoms, radiolarians, and planktonic foraminifers. Age assignments were primarily made on core-catcher samples. However, additional samples from within the core were studied when a core-catcher sample was found to be inconclusive or otherwise unrepresentative of the core in its entirety. Additional age determinations based on calcareous nannofossils were obtained by shore-based studies (C. Müller).

In general, a precise biostratigraphy is very difficult due to low-diversity assemblages of all fossil groups caused by dominantly cold water temperatures. Other factors responsible for the scarcity of the fossils are dissolution, recrystallization and dilution by the high input of detrital material. The age determination given for the Leg 141 sequences are based on the different biostratigraphies summarized and correlated in Figure 10.

Diatoms

The diatom zonation employed for Leg 141 is that proposed by Barron (1985), Barron, Keller, et al. (1985), and Barron, Nigrini, et al. (1985).

Age (Ma)	Series	Nanno-plankton zones	Foraminifer zones		Radiolarian zones	Diatom zones
			Low Latitudes	High		
0.25	Pleistocene	upper	NN21	T. truncatulinoides (T. tos) T. trunc	RN16 B. invaginata	Pseudoeunotia doliolus
0.45		NN20	RN15 C. tuberosa			
0.65	lower	NN19	T. truncatulinoides	G. inflata	RN14 A. ypsilon	Nitzschia reinholdii
1.6	upper	NN16–18	G. miocenica T. tosaensis		N. pachyderma sinistral	
3.2	lower	NN15	G. margaritae G. crassaformis	Rn11 S. pentas		Nitzschia jouseae
3.4						

Figure 10. Biostratigraphic zonal schemes used for Leg 141.

Each core-catcher sample (a few cm³ of sediment) was processed in a 400-mL beaker with hydrogen peroxide and hydrochloric acid. The solution was heated until the boiling reaction of the hydrogen peroxide stopped. The sample was then suspended in approximately 300 mL distilled water and decanted after a settling time of 2 hr, removing clay-sized particles still in suspension. The cleaning process was repeated until the acid was neutralized and a pH of approximately 6 was reached. Strawn slides of acid-cleaned material were prepared on 22 × 50 mm cover glasses and mounted on glass slides using Hyrax as the mounting media. Each slide was examined at a magnification of 500× for the presence of biostratigraphic marker species. The identification of marker species was routinely checked at a magnification of 1250×.

A semiquantitative approach was utilized to estimate abundances for specific species, and fragmented diatoms were treated according to the counting convention proposed by Schrader and Gersonde (1978). The approximate abundance classification used is based on observed occurrences at the magnification of 500× and are as follows: A = abundant, two or more specimens present in a field of view; C = common, one specimen encountered in two fields of view; F = few, one specimen observed in one horizontal traverse across the slide; R = rare, less than one specimen observed in one horizontal traverse; B = barren, no diatoms encountered.

The preservation of diatoms in each sample was classified according to three major categories based on evidence of dissolution and the presence of complete, broken, or thinly to heavily silicified valves. The following classification was used: G = good, specimens well preserved, thinly silicified valves present, none or only minor signs of dissolution; M = moderate, some thinly silicified valves present, slight to moderate signs of dissolution; P = poor, only heavily silicified valves present, abundant broken specimens, severe dissolution.

Radiolarians

The low-latitude radiolarian zonation of Sanfilippo, et al. (1985) was primarily employed during Leg 141. Sequential numbers (Fig. 10) are designated for each of the corresponding zones, following the practice of ODP Leg 130 (Kroenke, Berger, Janacek, et al., 1991).

Whenever necessary, we used the high-latitude zonation of Lazarus (1990, 1992) which partially incorporates zonations initially proposed by Hays (1965) for the Pliocene-Pleistocene, Chen (1975), and Caulet (1991) for the middle Miocene through early Pliocene.

Samples were prepared from 20 cm³ of sediment, with 30% H₂O₂, 10% HCl, and 1% Calgon solutions. Shipboard strawn slides were made from the size fraction >63 μm. Additional slides were prepared onshore to locate biostratigraphic events more accurately within the core. The abundance recorded is based on qualitative examinations of the prepared microslides. The following criteria were used to designate abundances of individual taxa: A = abundant (>100 specimens); C = common (50–100 specimens); F = few (10–50 specimens); and R = rare (<9 specimens). The preservation states of radiolarians were defined as follows: G = good (no sign of dissolution); M = moderate (minor dissolution); and P = poor (strong dissolution).

Foraminifers

Planktonic foraminifers observed in the Chile Triple Junction sequences are intermediate to those described from low latitudes (Blow, 1969, 1979; Bolli and Saunders, 1985; Kennett and Srinivasan, 1983) and those known from mid- and high-latitudes of the Subantarctic Regime (Srinivasan and Kennett, 1981; Jenkins, 1985). However, it is possible to recognize the *Truncorotalia*

truncatulinoides Zone, the *T. truncatulinoides*/*T. tosaensis* overlap Zone, the *T. tosaensis* Zone, the *Globoconella inflata* Zone, and the *Globorotalia crassaformis* Zone. It seems the zones are ecozones mostly influenced by temperatures. Age assignments are difficult and tentative. Further investigations are warranted.

Temperature is one of the habitat controlling factors of foraminifer distribution in modern oceans. The taxa of planktonic foraminifers can be roughly divided into warm-water assemblages and cold-water forms. The majority of the Holocene planktonic foraminifers live in tropical and subtropical waters, whereas only a single species, *Neogloboquadrina pachyderma* (sinistral coiling form), lives in polar waters. The regions where warm-water and cold-water assemblages overlap in distribution and where the greatest faunal contrast occur are designated as Transition Zones (Bé and Tolderlund, 1971). The area under the present investigation falls in the Southern Transition Zone of Holocene planktonic foraminifers, bounded by the Subtropical Zone in the north and by the Subantarctic Zone in the south. While subtropical/tropical and subpolar species of foraminifers do occur together in transitional waters, only *G. inflata* appears to be indigenous to, and a good indicator species of the Transition Zone (Bé and Tolderlund, 1971).

The assemblages of benthic foraminifers were mainly governed by water masses and nutrients. Benthic foraminifers are good indicators of ecology, bathymetry, transport, and of resedimentation processes in the oceans. Benthic foraminifers off Peru, the eastern South Pacific, have recently been studied by Resig (1990). Coastal benthic foraminifers off Chile have been studied by d'Orbigny (1839), Brady (1884), Boltovskoy (1976), and Boltovskoy and Theyer (1970). To reconstruct paleoenvironments, depth-ranges of benthic foraminifers summarized by van Morkhoven et al. (1986) and Resig (1990) were used. To characterize biotopes, the following depths were used: 0–200 m water depth = neritic environment, 200–500 m = upper bathyal, 500–2000 m = middle bathyal, 2000–4000 m = lower bathyal, and > 4000 m water depth = abyssal environment (Resig, 1990).

To study planktonic and benthic foraminifers, the same samples were used. The preparation methods used to obtain foraminifers were the standard techniques: briefly, the samples were soaked in diluted H₂O₂ solution, washed over a 63-μm screen, dried, and the fossils were separated under the binocular microscope. For calculating abundances in rich samples, the specimens of foraminifers were separated by down-splitting the whole residue. Poor samples were picked out totally. The planktonic/benthic ratios were calculated. In the range charts the abundances are categorized as A = abundant, more than 50%; C = common, 10%–50%; F = few, 1%–10%; R = rare, less than 1%; and B = barren. The state of preservation of planktonic foraminifers is described as follows: G = good, little or no fragmentation, overgrowth and/or dissolution; M = moderate, some signs of fragmentation, overgrowth and/or dissolution; P = poor, severe fragmentation, heavy overgrowth and/or dissolution.

Calcareous Nannofossils

Age determinations given by calcareous nannofossils are based on the standard nannoplankton zonation (Martini, 1971; Martini and Müller, 1986). Due to the scarcity or absence of zonal markers the biostratigraphic resolution is rather low.

STRUCTURAL GEOLOGY

Introduction

Structural geology was an important facet of visual core description on Leg 141. The priorities set by the structural geologists were:

LEG 141. Structural Data: Working Core Sheets.

Hole 863A		Core 411		Observer QSO		Comments		
section	cm from top	X-Ref	ID	thicknes	Core Face Orientation	Calc Orientation	Calc Orientation	Description, sketches, other data
	top	bottom		cm	App Dip	Core Ref Frame	Geog Ref Frame	
2	6	7	(19) B		60	90	2 60E	W UP CORE E
"	6	10	(20) Fu		34	290	181 34W	
"	15	21	(21) "		47	90	7 47E	
"	60	66	(22) "		30	270	179 30N	
"	60	67	(23) "		60	270	182 60W Normal	
"	65	70	(24) "		45	270	182 45W Contact	
"	68	70	(25) "		12	70	355 12E Parallel to B.P.	
"	68	70	(26) "		33	90	9 33E Normal	
"	74	78	(27) "		16	90	14 16E Contact	
"	78	84	(28) "		63	70	19 63E Normal	
"	83	84	(29) "		40	90	11 40E Parallel to B.P.	
"	85	96	(30) "		45	70	3 45E Normal	
"	101	102	(31) "		41	270	178 41W Reverse	
"	103	103	(32) "		31	90	11 32E Parallel to B.P.	
"	105	108	(33) "		50	270	176 50W	
"	107	112	(34) "		1	270	98 75 contact	
"	110	114	(35) "		47	90	357 47E Reverse	
"	115	112	(36) "		31	270	188 31W contact	
"	112	125	(37) "		70	270	170 70W (1)	
"	130	135	(38) "		46	270	175 46W Normal	
"	133	137	(39) "		57	90	5 57E Contact	
"	136	140	(40) "		53	270	195 53W Reverse	
3	13	15	(41) "		70	270	176 70W Parallel to B.P.	
"	18	20	(42) "		2	270	112 55	
"	25	27	(43) "		50	270	192 51W Reverse (apparent normal) exists	
"	35	43	(44) B		61	270	182 61W	
"	35	43	(45) Ft		46	90	336 46E Reverse	
CL	10	12	(46) "		9	270	192 9W Normal (low angle, apparent)	

Figure 12. An example of the working core description sheet found useful for recording structural features. The original form measures 40 x 28 cm, occupying two joined U.S. letter-size (11 x 8 1/2 in.) sheets.

away from working half). These data were not recorded permanently but used to calculate true dips in the core reference frame. True dips were calculated stereographically on a computer using the stereonet plotting program of R.W. Allmendinger, Version 4.1-11, on a Macintosh computer. The two apparent dip orientations were entered as lines, and the computer found the great circle of cylindrical best fit to both lines. The orientation of this great circle gave the true orientation in the core reference frame of the observed structure, which was recorded on the description form and also entered into the spreadsheet. Where a structure was seen as a three-dimensional plane in a fragmented piece of core, or its trace could be observed at the top or bottom of a core section, it was possible to measure the true orientation directly in the core reference frame. The convention shown in Figure 15 was adopted, where 000° (a "pseudo-north") is the direction that splits the archive-half at right angles and goes from the exposed face to the single line on the core liner. Because the structural descriptions are based on the archive-half of the core, it was found more convenient to define the reference frame with respect to that half rather than the working half used in some other conventions.

At the top and bottom of the core and on broken pieces, it was occasionally possible to discern linear structures such as the hairline grooves associated with faults and shear bands, called

here slickenlines. The orientations of these and all other lineations were recorded. Fold axes were measured, where possible, by excavating the nose of the fold in the working half so that a pin could be passed through two equivalent inflection points on two orthogonal surfaces (Fig. 16A). The orientation of the pin was then recorded as a pitch on a plane containing the pin line and the N-S horizontal line in the core reference frame (Fig. 16B). The plane and pitch were entered into the stereo-plotting program and the plunge and plunge direction of the fold axis in the core reference frame read off.

The sense and magnitude of fault separation was routinely recorded as it appeared on the core face or on the tops of broken pieces. Dip-slip separations and magnitudes were measured on the core face and referred to as normal or reverse movements. Strike-slip separations were measured on top surfaces and termed sinistral or dextral. Wherever possible, two observed separations were combined, or one separation and an observed slickenline orientation were combined, to calculate the true motion vector and displacement. In some cases, several cuts were made to better constrain the true displacement values of the faults.

Our measurements of the orientations of structures observed in the cores were facilitated by a simple tool suggested by Neil Lundberg. A more detailed description of the tool and its use can

LEG 141. Structural Data: Summary Spreadsheet for Site 859

Site 859A																				
core	section	cm from top		mbsf	X-Ref	Photo?	ID	identifier	thickness	Core Face Orientation		Core Ref frame			Reorient	Geographic Ref frame			Use these columns to add extra data as it becomes relevant	
		top	bottom							App Dip	Direction	Strike	Dip	Dir		Method	Strike	Dip		Dir
		Hand Sheets																		
1H	1			0	NIL															
1H	CC			1	NIL															
2H	1	97	99	2.17	1	B	Bedding		18	270	135	25	W	Palaomag	217	25	W	Remanent magnetism after 15mT		
2H	2	23	26	2.93	1	Fo	Fold	2												
2H	2	24	25	2.94	1	Fap	Axial Plane		16	270										
2H	2	37	50	3.07	2	B	Bedding		0	0										
2H	2	78	83	3.48	3	B	Bedding		16	270										
2H	2	122	126	3.92	4	B	Bedding		30	27	203	32	W	Palaomag	285	32	N			
2H	2	146	149	4.16	5	B	Bedding		50	270										
2H	3	10	12.5	4.3	1	B	Bedding		25	270	180	25	W	Palaomag	262	25	N			
2H	3	30	36	4.5	2	B	Bedding		24	270	180	24	W	Palaomag	262	24	N			
2H	3	72	72	4.92	3	B	Bedding		0	90	90	6	S	Palaomag	172	6	W			
2H	3	74	74	4.94	4	Fo	Fold	0.5												
2H	3	96	102	5.16	5	B	Bedding		34	270	202	36	W	Palaomag	284	36	N			
2H	3	111	116	5.31	6	B	Bedding		48	270										
2H	4	8	12	5.68	1	B	Bedding		0	0	0	0		Palaomag	82	0				
2H	4	109	112	6.69	2	YES	F	Fold	2											
2H	4	109	112	6.69	2	YES	Fax	Fold Axis										14/235 Fold axis reorients to 14/317		
2H	4	109	112	6.69	2	YES	Fap	Axial Plane	8	90	78	33	S	Palaomag	160	33	W			
2H	4	111	115	6.71	3	B	Bedding		18	90	320	23	E	Palaomag	222	23	E			
2H	5	9	9	7.19	1	B	Bedding		3	270	103	13	S	Palaomag	185	13	W			
2H	5	26	27	7.36	2	B	Bedding		9	90	59	17	S	Palaomag	141	17	W			
2H	5	102	103	8.12	3	B	Bedding		5	270										
2H	6	16	17	8.76	1	B	Bedding		4	90	84	34	S	Palaomag	166	34	W			
2H	6	26	27	8.86	2	B	Bedding		7	270	125	12	S	Palaomag	207	12	W			
2H	6	104	105	9.64	3	B	Bedding		2	270	117	4	S	Palaomag	199	4	W			
2H	7			10.1			NIL													
2H	CC			10.6			NIL													
3H	1	21	23	10.91	1	B	Bedding		7	90	325	9	E	Multishot	202	9	N	Double line towards 043° Magnetic		
3H	1	21	23	10.91	1	B	Bedding		30	90										
3H	1	121	128	11.91	2	B	Bedding		50	90	358	50	E	Multishot	235	50	N			
3H	1	124	125	11.94	3	B	Bedding		19	96	27	21	E	Multishot	258	21	N			
3H	2	24	25	12.34	1	B	Bedding		10	270	169	10	W	Multishot	46	10	S			
3H	2	55	62	12.65	2	B	Bedding		53	270	156	55	W	Multishot	33	55	S			
3H	2	94	107	13.04	3	B	Bedding		85	270										
3H	2	108	117	13.18	4	B	Bedding		73	270	174	73	W	Multishot	51	73	S			
3H	3	110	135	14.6	1	YES	CV	Clastic Vein?	4	84	90	0	84	E	Multishot	321	84	N	Some concern over origin	
3H	3	134	136	14.84	2	YES	F	Fault	12	270	150	14	W	Multishot	27	14	S	Must be tectonic, perhaps gravity glide		
3H	4	60	150	15.6	1	YES	CV	Clastic Vein?	2.5	90	90	0	90	W	Multishot	327	90	S	En echelon. Possibly drill related?	
3H	CC	0	24	16.5			CV	Clastic Vein?	2.5									Continuation of section 4.		
4H	1			#VALUE!	NIL															
4H	2			#VALUE!	NIL															
4H	3			#VALUE!	NIL															
4H	4			21.1	NIL															

Figure 13. An example of the spreadsheet devised for the computer storage and manipulation of structural data derived from the core descriptions. The original measures 25 cm × 17 cm and occupies a U.S. letter-size sheet. The example includes the data shown in Figure 11.

Structural identifiers						
Identifier		Planar component		Linear component		Comments
Bedding	B	Bedding surface	B			Identified by change in color, composition, grain size.
Fabrics		Foliation		Lineation		Includes grain alignment, shape fabric, fracture cleavage (FC).
Folds	Fo	Fold axial surface	Fap	Fold axis	Fax	
Faults	F	Fault plane	F	Slickenline	SI	Any discrete planar break showing a displacement. Where possible dip separations (normal or reverse) are recorded in the core-face, and strike separations (dextral or sinistral) on the core ends.
Deformation band	DS	Deformation band				Planar or curvilinear feature recognized in core as a seam or seams of different color or grain size and attributed to deformation. Includes features which may also be called faults, together with shear bands, shear zones, kinks, etc.
Mineral veins	V	Mineral veins	V			Openings filled with mineral or minerals such as calcite, quartz, or pyrite.
Clastic veins	CV	Clastic veins				Mode 1 fractures filled with clastic sediment.
Breccia	B					Sedimentary breccia (SBr), Fault breccia (FBr).

Figure 14. Terminology of structural identifiers used for structure observed in core during Leg 141.

be found in the Explanatory Notes to Leg 131 (Taira, Hill, Firth, et al., 1991). The device is illustrated in Figure 17A. It consists, in principle, simply of a protractor-like graduated scale with a pivoted measuring arm. During measurement, one half of the arm is aligned closely against the structure of interest and the other half points to the value of the dip angle on the graduated scale.

Figure 17B shows the device being used to measure the apparent dip angle of a structure on a split core face, a very common application. Dip angles refer, by definition, to inclinations from the horizontal, but there is no horizontal datum on a core; rather, it is the vertical axis, the length of the core, that forms the obvious datum. The baseline of the clinometer is therefore aligned vertically. With the device in this alignment, the arrangement of the graduated scale is such that when the measuring arm is rotated from horizontal to vertical the readings increase from 0° to 90°. *Note that this is the opposite arrangement from that found on a conventional protractor. The device as suggested here therefore reads the dip angles directly, eliminating the mental arithmetic necessary if it is constructed from an ordinary protractor.*

The advantages of the tool apply equally to measuring a dip angle at right angles to the core face (Fig. 17C), or on some surface along which the core has broken. The instruments available on Leg 141 were too large for this application because the measuring arm hits the core table except when measuring shallow apparent dips. Azimuth of features may be measured by aligning the baseline of the device with the split core face, and positioning the arm parallel to the feature (Fig. 17A).

The arrangement of the scale is correct for the core reference frame used on Leg 141 provided the azimuths fall in the “north-east” quadrant; those falling in the “northwest” quadrant will require the reading to be subtracted from 360°.

Real Orientation of the Structures

Following the recording of orientation data on the descriptive sheets as outlined above, it is necessary to convert these local orientations to geographical coordinates. The multishot and tensor technique allows piston cores to be oriented with respect to magnetic north, and hence the arbitrary local reference frame to be positioned. The paleomagnetic approach was also employed, provided the core material was reasonably consolidated. It was especially useful for cores obtained by rotary (RCB) and extended core barrel (XCB) drilling because these techniques often cause the core to break into several pieces that rotate independently of each other within the core liner. To remove these drilling-induced rotations, paleomagnetic information was gathered from sections of core that were considered to be structurally continuous, that is, rotated as a single piece. The magnetic data, obtained by the cryogenic magnetometer from the demagnetized archive halves of the cores, were also routinely collected and stored in the paleomagnetic lab. With the aid of the on-board paleomagnetic specialists, we found it possible to apply this information to the structural measurements. To obtain the data from samples shorter than the averaging limits of the cryogenic magnetometer—typically this would apply to pieces less than 10 cm in length—the individual pieces were removed from the working half of the core and run through the instrument without demagnetization. Both methods provided the declination and inclination of the natural remanent magnetism in the sample, which could then be used for orienting the structures. The details of orientation methods used for specific cores are discussed in the site chapters.

Core pieces were often reoriented relative to each other, although not necessarily in a geographic reference frame, by com-

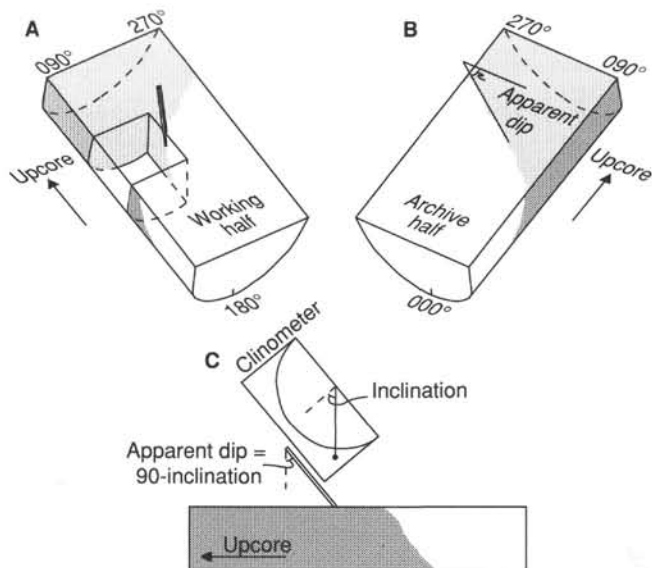


Figure 15. Diagram to show the conventions used for measuring azimuths and dips of structural features in core and the techniques adopted for measuring structural planes in three dimensions in the core reference frame. The core reference frame conventions for the working half and the archive-half of the core can be seen in (A) and (B). The E-W (core reference frame) apparent dip of a feature was measured first, generally on the face of the archive-half (B). The data were recorded as an apparent dip toward either 090° or 270°. In this case the apparent dip is toward 090°. A second apparent dip is measured by making a cut parallel to the core axis but perpendicular to the core face in the working half of the core (A). Note that cuts were normally considerably smaller than the one represented in the diagram. The feature is identified on the new surface and the apparent dip in the N-S direction (core reference frame) marked with a toothpick. The apparent dip is measured with a clinometer (C) and quoted as a value toward either 000° or 180°. In this case the apparent dip is toward 180° (into the working half). True dip and strike of the surface in the core reference frame are calculated from the two apparent measurements.

paring the relative orientations of certain structures from one piece to the next. Examples of this technique are explained more completely in the Structural Geology section of Sites 860 and 862 chapters.

PALEOMAGNETISM

Paleomagnetic studies on Leg 141 involved the measurement of natural remanent magnetization (NRM) on both complete sections from the archive-half of the split core and discrete samples taken from the working half, and remanence after stepwise alternating field (AF) demagnetization. Bulk magnetic susceptibility was routinely recorded as part of the suite of MST measurements.

Zones of normal and reversed polarity were interpreted from the continuous archive-half measurement, supplemented by discrete samples. Magnetic polarity data were integrated with biostratigraphic data to construct a magnetostratigraphy, which was correlated with the magnetic polarity time scale of Berggren et al. (1985; see Biostratigraphy section, this chapter). More detailed and extensive demagnetization of the discrete samples was possible than for the continuous sections; the demagnetization behavior of the discrete samples clarified the interpretation of the magnetic record in the continuous sections. Mean directions for the primary remanence and viscous remanent magnetization (VRM) were used by the structural geologists to orient structural features (see Structural Geology section, this chapter).

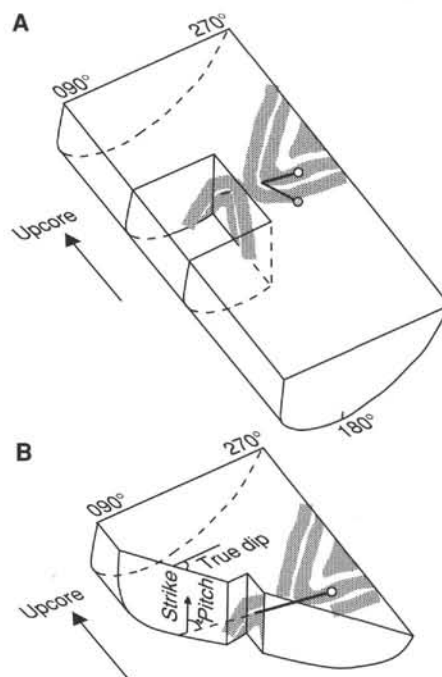


Figure 16. Procedure for measurement of a fold axis orientation in core. A cut was made parallel to the core axis but perpendicular to the core face in the working half of the core (A) to expose the fold nose. Note that cuts were normally considerably smaller than the one represented in the diagram. The same inflection point exposed in the two exposed surfaces was then pierced with a pin. The orientation of the pin in the core reference frame, and hence of the fold axis, was measured as a pitch on the plane containing the pin and the N-S horizontal line. This plane has been schematically exposed in B. As the plane contains the N-S horizontal line, the apparent dip measured on the core face is also the true dip. The strike of the plane is either 000° or 180°. The convention in the Allmendinger stereoplot program requires the strike closest to the pitch to be quoted, together with a dip and dip direction, and the value of the pitch. In practice the pitch of the pin was measured by lining up a stiff board with the plane containing the pin and the N-S horizontal line and measuring the inclination of the pin parallel to this board. The pitch is then 90°—the measured inclination.

Remanent Magnetization Measurements

Measurement and Demagnetization

Measurement of remanence in complete sections from the archive-half of the core was conducted with a 2-G Enterprises (model 760R) pass-through cryogenic rock magnetometer. An AF demagnetizer (Model 2G600) capable of alternating fields up to 20 mT is aligned along axis with the magnetometer; demagnetization of the archive-half sections was normally limited to 15 mT or the mean destructive field, whichever was less, in accordance with ODP policy. Both the cryogenic magnetometer and the AF coils are encased in a mu-metal shield, and an automated sample-handling system moves the core sections through the AF coils and the magnetometer sensor region. The cryogenic magnetometer, AF demagnetizer, and sample-drive system are controlled through a Baytech communication board by an IBM PC-AT compatible computer. Measurements and demagnetization passes using the cryogenic magnetometer were operated by a modified version of a University of Rhode Island BASIC program.

The superconducting quantum interference device (SQUID) sensors in the cryogenic magnetometer measure magnetization over an interval approximately 20 cm long. The widths of the

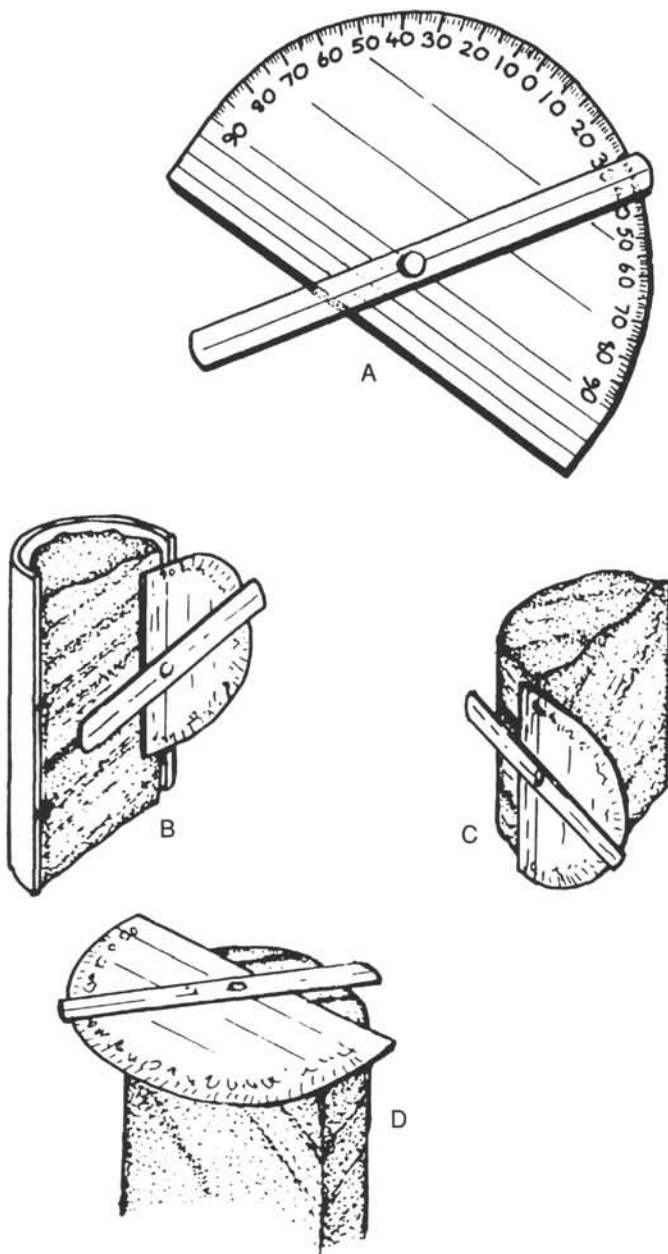


Figure 17. A. Drawing of a device for measurement of core-structure orientations. B. Device being used to measure the dip of a structure on the face of a split core. C. Device being used to assess the dip of a structure as seen at right-angles to the split-core face. D. Measurement of the azimuth of a structure as seen on an upper surface of a core.

sensor region suggest that as much as 150 cm^3 of core contributes to the output signal. The large volume of core material within the sensor region allows accurate determination of remanence for weakly magnetized samples despite the relatively high background noise related to the motion of the ship. The cryogenic magnetometer is incapable of measuring archive-halves with a magnetization greater than 1 A/m ; intensities of this magnitude generate too many flux jumps for the SQUID sensors to consistently track.

Remanence measurements were performed by passing continuous archive-half core sections through the cryogenic magnetometer. Remanence measurements were taken at intervals of

either 5 or 10 cm along the core, both for NRM and after AF demagnetization at 5, 10, and 15 mT.

Discrete samples in soft sediments were sampled either as standard ODP "cubes" (plastic boxes shaped as square prisms with a volume of 5.6 cm^3) or "French cubes" with a volume of 8 cm^3 . Both types of cube have an arrow on the split face pointing upcore. Semilithified sediments were cut to fit the boxes with two parallel saw blades; lithified sediments were prepared as 10 cm^3 "minidrill" cylinders with a water-cooled drill press. Discrete samples were sometimes measured in the cryogenic magnetometer. To do so they were placed in a halved core liner specially modified to carry the discrete samples and run through the magnetometer/demagnetization unit using a modified version of the controlling program. Other discrete specimen measurements were conducted on a Molspin spinner magnetometer, semiautomatically controlled by the ODP-developed Macintosh application "MolMag."

Discrete samples run through the cryogenic magnetometer were demagnetized up to 20 mT by the on-line AF coils. Higher AF demagnetizations for these samples, and all AF stages for samples measured on the spinner magnetometer, were conducted using a single-axis Schonstedt geophysical specimen demagnetizer (Model GSD-1). When the single-axis device was used, three mutually orthogonal demagnetization runs were carried out for each AF level. All demagnetization and measurements were performed within mu-metal shields; discrete samples reserved for shipboard analysis were also stored within a triple-layered mu-metal cylinder.

Data Analysis

Demagnetization data for the discrete samples were graphically analyzed by their presentation as Zijdeveld orthogonal demagnetization plots (Zijdeveld, 1967). Mean magnetization directions and statistics were calculated according to the method of Fisher (1953).

Orientation

Measurements were made relative to X, Y, and Z axes defined as depicted in Figure 18. In extended core barrel (XCB) and rotary core barrel (RCB) cores the free rotation of the core during recovery removes any external control on the geographic orientation of the X and Y axes; only the Z (down) axis, and hence inclination, has a consistent meaning from core to core or between discontinuous lithified pieces. Geographic orientation of the X-axis for hydraulic piston cores (APCs) was determined by two devices during Leg 141. At Site 859 a conventional photographic Eastman-Whipstock Multishot Tool, well established in ODP usage, was used in tandem with a modified Tensor "Champ" three-axis fluxgate magnetometer. This test established the reliability of the Tensor tool, which was used alone at subsequent sites. In its configuration for Leg 141 the modified Tensor tool did not contain accelerometers to establish the hole inclination; the Eastman-Whipstock Multishot tool did measure hole inclination, but this has not been taken into account in past studies. Hole inclination in APC coring can be expected to be less than 5° , so the assumption that the holes are vertical should not have introduced errors in declination greater than about 10° at the latitude of the Leg 141 sites.

Working in reverse, the orientations of viscous remanences (VRMs) and of primary magnetizations were used to establish current and paleo-norths, and the original horizontal of inclined sediments, in some of the otherwise unoriented XCB and RCB cores. This work was carried out jointly with the structural geologists and allowed absolute orientation of a number of structural features (see Structural Geology section, this chapter).

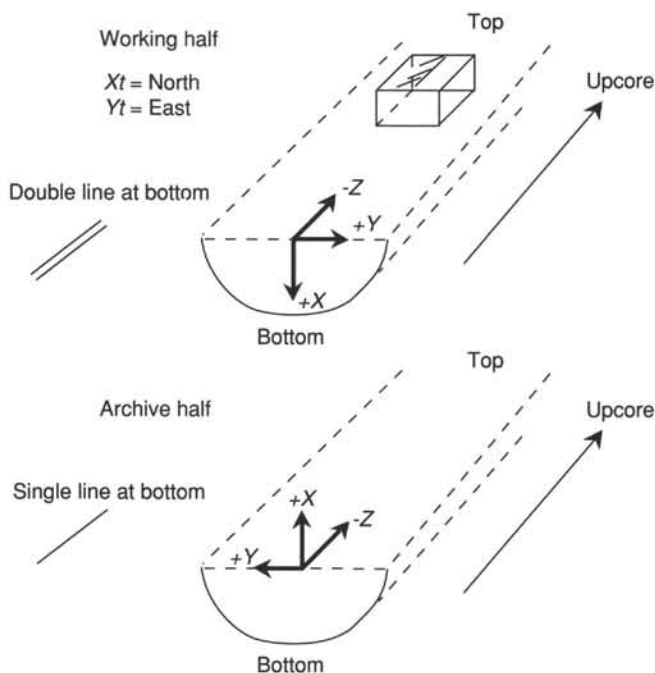


Figure 18. ODP magnetic direction conventions.

Magnetic Susceptibility Measurements

Whole-core magnetic susceptibility measurements were made on all cores using a Bartington Instruments magnetic susceptibility meter (model M.S. 1) with an M.S. 1/CX 80-mm whole-core sensor loop set at 0.47 kHz. The susceptibility meter is part of the MST, which also contains a gamma-ray attenuation porosity evaluator (GRAPE) and *P*-wave logger (see Physical Properties section, this chapter). Because magnetic susceptibility is a temperature-dependent property, the cores were permitted to thermally equilibrate (usually for 4 hr) prior to the analysis on the MST.

ORGANIC GEOCHEMISTRY

The following instrumentation and procedures were used during Leg 141 (1) to measure the concentrations of hydrocarbon and other gases, (2) to test for gas hydrates, (3) to conduct analysis of high molecular weight hydrocarbons in selected sediments, and (4) to determine the quantity and quality of organic matter in the sediments. These procedures were carried out for safety considerations and to provide preliminary information for more detailed shore-based studies.

Hydrocarbon and Other Gases

Compositions and concentrations of hydrocarbon and other gases were measured using two different gas chromatographs: Hach-Carle AGC Series 100 (Model 211), referred to as HC, and Hewlett-Packard 5890A, Natural Gas Analyzer, modified by John Booker & Company, Austin, Texas, and referred to as HP.

Hach-Carle Gas Chromatograph (HC)

The HC was attached to a Hewlett-Packard Model 3393A Integrator that allowed the single measurement of gas concentrations over six orders of magnitude after appropriate calibration. The HC instrument is designed to measure accurately and rapidly the concentrations of methane, ethane, and propane, taking about 7 min. Ethene is resolved from ethane and can also be quantified. The HC has the following characteristics: sample introduction

was via a 1.0-cm³ sample loop with manual column backflush; the chromatographic columns used were a 0.32 cm × 1.8 m stainless steel tubing packed with 80% Poropak N and Poropak Q (80/100 mesh) and a 0.32 cm × 1.8 m stainless steel tubing packed with 10% Carbowax 20M on Chromasorb W-HP (80/100 mesh). Only the first column was used for routine analyses. For detection a flame ionization detector was used and the chromatographic conditions were isothermal at 90°C, with helium used as the carrier gas.

Hewlett-Packard Gas Chromatograph (HP)

The modified natural gas analyzer is a Hewlett-Packard, Model 5890a modified gas chromatograph (GC) equipped with both a thermal conductivity detector (TCD) and a flame ionization detector (FID). Four automatic switching valves are controlled by a Hewlett-Packard Model 3393A Integrator that also monitors the TCD. A second integrator of the same model monitors the FID. This analysis system provides a rapid capability to determine N₂, O₂, CO, H₂S, CS₂, and the hydrocarbon gases from methane to at least the heptanes.

The modified natural gas analyzer (HP) chromatographic system employs a multicolumn system composed of: a 0.32 cm × 1.8 m stainless steel column packed with Poropak T (50/80 mesh) in line with a 0.32 cm × 0.9 m column packed with Molecular Sieve 13X (60/80 mesh); a 0.32 cm × 1.8 m stainless steel column packed with 80/100 mesh Haysep (acid washed); and a 60 m × 0.32 mm capillary column coated with a 1-μm film thickness of DB-1 (J&W Inc.). An appropriate automatic valve switching system, controlled by the two Hewlett-Packard Integrators, allows the columns above to be used sequentially to provide the required chromatographic separation of C₁ to C₇ hydrocarbons and provide also the required backflush to eliminate heavier compounds if present. Samples were introduced via a 0.5 cm³ sample loop with automatic sample backflush. The chromatographic separation on the TCD portion of the Hewlett-Packard GC system was carried out isothermally at 80°C, whereas the hydrocarbon separation on the FID portion of the GC system was carried out by programming from 80° to 100°C at 8°C/min and then to 200°C at 30°C/min. Helium was used as the carrier gas. The TCD injector and detector temperatures were 80° and 150°C, respectively, and the corresponding temperatures for FID were 150° and 250°C, respectively. Chromatographic response was calibrated against preanalyzed standards and concentrations are reported in ppm (v/v).

During Leg 141, the compositions and concentrations of hydrocarbons and other gases were monitored in the sediments at intervals of generally once per core. Two methods were used, called headspace (HS) and Vacutainer (V).

In the HS method, gases released by the sediments after core recovery were analyzed with the following technique: a measured volume of sediment, usually about 3 cm³, was placed in a 23-cm³ glass vial that was closed with a septum and metal crimp seal. The vial was heated to 60°C in an oven and kept at this temperature for 30 min prior to gas analysis. A No. 6 cork borer with a calibrated plunger was used to obtain a measured volume of sediment from the end of a section of core as the core was processed on deck immediately after retrieval. Wherever lithified samples were encountered, chips of rocks were placed in the vial, sealed, and heated as above. A 5-cm³ volume of the headspace in the vial was removed for each analysis by gas chromatography (HC and HP).

A second headspace technique was used occasionally to obtain a larger gas sample for on-shore analysis. In this technique, a measured length (approximately 5 cm) of whole-round core, obtained immediately as the core was processed on deck, was placed in a paint can, previously prepared with two septa-covered entry ports, along with enough degassed water so that a 100-cm³ head-

space remained when the can was sealed. This headspace was purged with He, after which the can was shaken, and gas was released into the He-filled headspace. About 5 cm³ of this headspace gas was removed for each analysis by gas chromatography (HP). The cans were then inverted and frozen.

The Vacutainer (V) method of gas analysis was used when gas pockets (expansion voids) occurred in cores as they arrived on deck. Vacutainers are pre-evacuated, sealed glass tubes (20 cm³). For the purpose of obtaining a gas sample, a special tool was employed to penetrate the core liner. This tool, equipped with a valve and needle, was used to transfer gas from the core into the Vacutainer. Portions of gas in the Vacutainer were analyzed by gas chromatography (HC and HP).

Gas Hydrates and the Pressure Core Sampler

One of the main objectives of Leg 141 was to establish experimentally the presence of gas hydrates in the area, to correlate their occurrence with geophysical data with a bottom-simulating reflector (BSR), and to determine their physical and chemical properties. Two pressure measuring systems were available for studying gas hydrates.

Laboratory System

In the laboratory the pressure measuring system (Parr Instrument Co.) consisted of a sample holder (23 cm³), a gauge block, a pressure gauge, and a manifold. This system was designed to measure the pressure and temperature resulting from gas hydrate disassociation, the composition of released gases and the inorganic geochemical properties of the resulting water. Because no solid gas hydrates were recovered during Leg 141, this system was not utilized.

Pressure Core Sampler

The pressure core sampler (PCS) is a coring system designed to retrieve core samples at bottom-hole pressures, and thus it can be useful in the recovery and study of gas hydrates. The PCS is completely compatible with the existing ODP bottom-hole assembly and is wireline retrievable, free-fall deployable, and hydraulically actuated. It consists of five subassemblies: latch, actuator, valve accumulator, ball valve, and detachable sample chamber. The sampler recovers a nominal 42-mm diameter sediment core, 0.86 m long, at pressures up to 10,000 atm. The PCS has been deployed previously on Legs 124, 131, and 139.

After the PCS was deployed and recovered, it was placed in a cooling jacket and attached to a gas manifold that was first used on Leg 139. This manifold was designed to measure the amount and composition of gases coming from the pressurized sample. The manifold was evacuated and gases were collected in thermostated gas cylinders (300 cm³). Recovered gases were measured by gas chromatography (HC and HP).

Hydrocarbons

Solvent-soluble organic material was analyzed by gas chromatography on a Hewlett-Packard Model 5890A gas chromatograph, equipped with a capillary column and split injection. Operating conditions for this instrument were as follows:

1. Column, HP Ultra 1 (Crosslinked Methyl Silicon Gum), 50 m × 0.2 mm × 0.11 μm film thickness.
2. Conditions, He, 400 kPa; Air, 200 kPa; and H₂, 150 kPa.
3. Temperatures, injector, 250°C; detector, 300°C; temperature program, initial at 30°C for 3 min, 10°C/min to 220°C, 4°C/min to 300°C, and then isothermal for 15 min.

For the analyses of high molecular weight hydrocarbons, a 3 cm³ sediment sample was taken from cores by means of a No. 6 cork borer,

equipped with a calibrated plunger. The samples were taken from section ends immediately next to the HS samples. Each sample was placed in a 4-dram (15 cm³) vial that had a Teflon-lined cap. The sample was macerated with 5 mL methanol, and then 3 to 5 mL *n*-hexane were added. This mixture was shaken and centrifuged at 2000 rpm. The hexane layer was removed by means of a disposable pipette into a 0.5-dram (2 mL) vial, and the hexane extract was evaporated to about 50 μL under a stream of He. A 1- to 8- μL sample was injected into the gas chromatograph. Identification of compounds was based on comparison of retention times with those of authentic standards.

Organic Matter

Organic Matter Type (Pyrolysis Methods)

Two pyrolysis systems were available on Leg 141 to evaluate the quality and quantity of organic matter. The standard system is the Delsi-Nermag Rock-Eval II plus total organic carbon (TOC). A new system is the Geofina Hydrocarbon Meter (GHM). Both systems use a whole-rock pyrolysis technique to identify the type and maturity of organic matter and to detect petroleum potential and oil shows in sediments. The Rock-Eval system involves a graduated temperature program that first releases volatile hydrocarbons at 300°C for 3 min, and then releases hydrocarbons from thermal cracking of kerogen as the temperature increases at 25°C/min from 300° to 600°C. The total volatile (S₁) and total pyrolytic (S₂) hydrocarbons were measured by a flame ionization detector and are reported in milligrams of hydrocarbon per gram of sediment. A maximum temperature (*T*_{max}) value is obtained that corresponds to the temperature at which kerogen yields the maximum amount of hydrocarbons during the evolution of S₂. During the pyrolysis cycle, CO₂ produced from organic matter is trapped from 300° to 390°C and analyzed in a thermal conductivity detector yielding S₃, reported as milligrams of CO₂ per gram of sediment. In addition, the previously pyrolyzed sample is oxidized to provide additional data needed for the automatic calculation of TOC.

The GHM is a gas chromatographic system based on the Varian 3400 series gas chromatograph that has been modified to include the GHM pyrolysis injector and corresponding valve configuration. The system employs three flame ionization detectors and two capillary columns (25 m, GC2 fused silica). The system generates S₁, the free hydrocarbons that are released from the injector at 300°C, and (S₂), the pyrolysis products that are generated by ramping the temperature of the furnace from 300° to 540°C at 25°C/min. The effluent from the furnace is split 20:1 so that the hydrocarbon distributions making up S₁ and S₂ can be examined by capillary gas chromatography. *T*_{max} of the S₂ peak is also determined. Rock-Eval and GHM parameters are used to calculate Production Index (PI) = S₂/(S₁ + S₂), and Petroleum Potential or Pyrolyzed Carbon (PC) = 0.083(S₁ + S₂). Sample size for both systems is typically 100 mg. Results are presented as tables and graphs.

S₂ provides an indication of the quantity of hydrocarbons that could be produced, should burial and maturation continue. *T*_{max} indicates the maturity of the organic material.

Fluorescence

Fluorescence of bitumen reflects the aromatic content of the hydrocarbons and is an approximate indicator of the evolution of the petroleum potential of a sediment (Curry, Moore, et al., 1982). For sediment samples, fluorescence observation can be indicative of oil impregnation.

Fluorescence observations were made on total methanol/*n*-hexane extracts of core samples, by dissolving the total bitumen extracts in 0.5 mL *n*-hexane and estimating fluorescence color and intensity under a UV lamp (Curry, Moore, et al., 1982). For

sediment samples one half of the split core was observed directly under the UV lamp for fluorescent spots and/or fluorescent stains.

Elemental Analyses

At Site 863 sediments were analyzed for inorganic carbon (in carbonate) and for total carbon, hydrogen, nitrogen, and sulfur. The total organic carbon (TOC) content of the sediments was then calculated by subtraction of the inorganic carbon content from the total carbon content. Sediments were freeze dried and ground in an agate mortar prior to analysis.

Total inorganic carbon was determined using a Coulometrics 5011 coulometer equipped with a System 140 carbonate carbon analyzer. Depending on carbonate content, 15 to 70 mg of ground and weighed sediment was reacted in a 2N HCl solution. The liberated CO₂ was titrated in a monoethanolamine solution with a color indicator, while the change in light transmittance was monitored with a photo-detection cell.

Total carbon, hydrogen, nitrogen, and sulfur were determined using a Carlo Erba 1500 CNS analyzer. Bulk samples were combusted at 1000° in an oxygen atmosphere with addition of vanadium pentoxide in tin foil sample holders, converting organic and inorganic carbon into CO₂ and sulfur to SO₂. These gases, along with the water and nitrogen which were also generated, were then separated by gas chromatography and measured with a thermal conductivity detector.

The pyrolysis methods also provide information on the type of organic matter through the hydrogen index ($[100 \times S_2]/\text{TOC}$), the oxygen index ($[100 \times S_3]/\text{TOC}$) and the S₂/S₃ ratio. The former parameters are normally referred to as HI and OI, respectively.

FLUID GEOCHEMISTRY

Interstitial water was obtained from sediments by squeezing and by in-situ extraction using the water sampling temperature probe (WSTP).

Squeezing

Interstitial waters were squeezed from whole-round sections of sediment cores 6 to 10 cm long that were cut from the cores as soon as they arrived on deck. Sediment from whole-rounds was immediately extruded from the core liner, scraped with a teflon-coated stainless-steel spatula to remove the outer, contaminated layer, and placed in a titanium squeezer similar to the steel squeezer designed by Manheim and Sayles (1974). Sediments were squeezed in a Carver hydraulic press at pressures up to 2.8 MPa. Interstitial water was collected directly from the squeezer into 10- or 50-mL all-plastic syringes, from which the various aliquots for analysis were filtered through an on-line, 0.2- μm , polysulfone filter mounted in a Gelman "acrodisc" disposable filter holder. No attempt was made to equilibrate the sample with the in-situ temperature before squeezing. Squeezed interstitial waters were designated "IW" samples.

In-Situ Extraction

Interstitial water was extracted in-situ with the WSTP tool (Barnes, 1988), which simultaneously measures sediment temperature (Fig. 19). The tool is lowered on the coring wire to the end of the drill string, where it locks onto an assembly just above the bit. While the tool descends, the hole is flushed with drilling fluid (usually surface seawater) with the bit just off bottom to keep the hole free of fill. After the sampler is latched into place, the bit is lowered into the bottom with the filter assembly projecting about 1 m past the bit. A time-operated valve opens and interstitial water is drawn under negative pressure through the filter and into the sampler.

The filter assembly has been lengthened to 22 cm and is narrower than an earlier version of the tool. These modifications

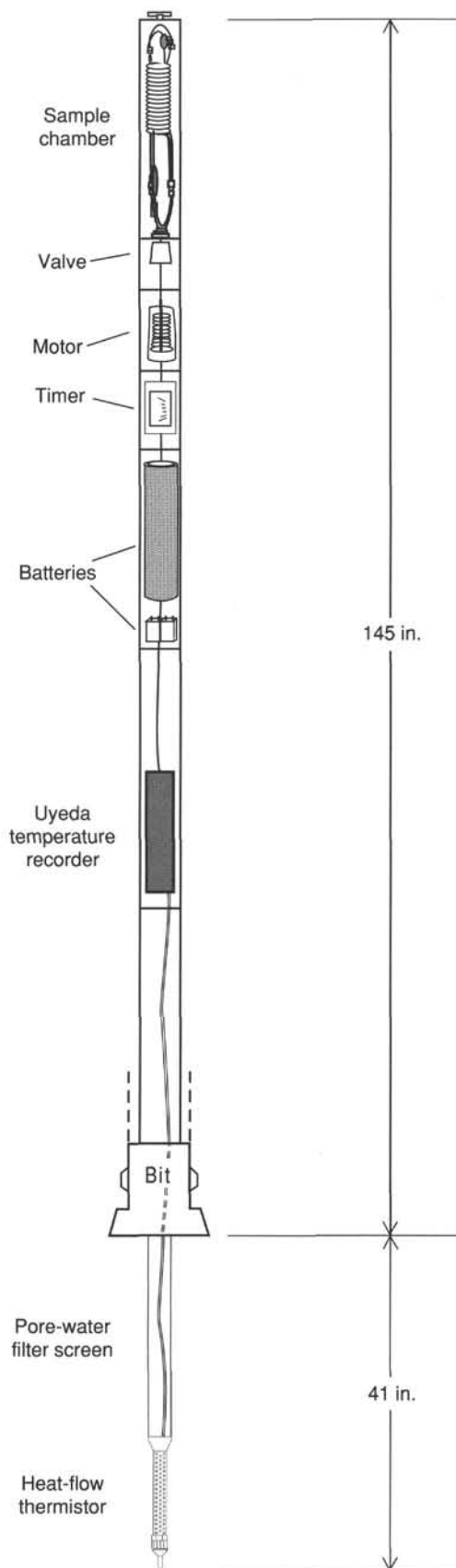


Figure 19. Schematic diagram of the WSTP sampler.

reduce fracturing of the formation and produce a filter surface area of 200 cm². A 1- μ m, polyester-mesh filter was sandwiched between two layers of 80- μ m titanium screen that were held together with epoxy. After passing through the filter assembly, pore fluids enter the sample reservoir via 1/16-in. titanium tubing. The tube is held in a groove cut into a titanium sleeve that fits around the thermistor probe shaft. The sleeve, tubing, and filter are covered by a second titanium sleeve. This outer sleeve provides support and abrasion protection for the filter and is perforated approximately every centimeter with 0.5-cm holes to allow fluid to pass. The titanium tube holds less than 4 mL of fluid and is connected to a titanium sample coil that holds approximately 6 mL of fluid. This in turn is connected to a copper sample coil that holds approximately 40 mL. Except for the copper coil, all of the connectors and valves are titanium or teflon. A one-way valve is connected to the other end of the copper coil, which allows fluid to pass into a stainless-steel overflow cylinder. This overflow cylinder generates negative pressure when the sampling valve is open, as this cylinder is normally filled with air when the tool is sent downhole. For Leg 141, we flushed this cylinder with nitrogen and evacuated it prior to deployment.

The procedure for fluid sampling with the WSTP is unchanged from that used during earlier legs. Prior to deployment the fluid path is back-filled with distilled water that has been previously degassed by bubbling nitrogen. The overflow cylinder is flushed with nitrogen and evacuated. A timer is set for a fixed time after which the valve will open, exposing the sampling line and chamber to ambient pressure. The timer also closes the valve after a prearranged time interval has passed. The length of time required to fill the WSTP is unknown, but the valve is kept open for about 10 min. The tool is recovered after the sample valve has closed.

When the tool is returned to the laboratory, the cover for the chamber containing the sample coils is carefully removed and any "overflow" water present is collected and designated as a "WO" sample. This fluid includes the distilled water that occupied the space inside the titanium tubing (6 mL) and the sample coils (54 mL) before deployment, plus all fluid in excess of 60 mL collected downhole. If a small fluid sample (<60 mL) is collected by the tool, the overflow fluid will be nearly all distilled water, and the sample will be diluted. If a large volume is collected (>60 mL), then the fluid trapped in the sample coils is from either the formation or the borehole. Fluids from the overflow cylinder also were analyzed, as they often are useful for determining the concentration of the major and minor species that are dissolved in pore waters. The amount of dilution of the overflow aliquot can usually be determined from its chlorinity relative to that of the undiluted sample. Whether the tool samples pristine, in-situ pore water depends on how deeply it is pressed into the formation, how permeable the sediments are, and whether the formation cracks during insertion of the probe.

Fluid from the titanium sample coil was filtered (0.2 μ m) and used for determination of major and minor dissolved species. These samples were designated "WT." The copper coil was hermetically sealed for later analysis of helium isotopes and dissolved gases. These samples were designated as "WC" samples.

Analytical Methods

Interstitial fluid samples were analyzed immediately upon recovery for pH, alkalinity by potentiometric titration, and salinity by refractive index. Aliquots were refrigerated and analyzed within a few days for chloride, magnesium, and calcium by colorimetric titration; sulfate by ion chromatography and turbidimetry; boron, silica, and ammonium by colorimetry; fluoride by an ion-specific electrode; potassium, sodium, and lithium by flame atomic emission, and strontium by atomic absorption spectrophotometry. Most shipboard analyses were performed using

standard ODP techniques, as detailed by Gieskes et al. (1991). The techniques employed are summarized in Table 1. We used IAPSO as our primary standard for determination of calcium, magnesium, chlorinity, and sulfate. Other analyses employed reagent grade chemicals as suggested by Gieskes et al. (1991).

IGNEOUS AND METAMORPHIC ROCKS

Core Curation and Shipboard Sampling

Prior to cutting, hard-rock samples were examined for structural orientations, and sediment-rock contacts were examined for chilled margins, baked sediment and alteration aureoles. Each contiguous piece was numbered sequentially from the top of each core section and labeled. Broken core fragments that could be fitted together were reassembled into pieces; each fragment was lettered consecutively from the top down (e.g., 1A, 1B, and 1C). Composite pieces often occupied more than one section. Plastic spacers were placed between pieces with different numbers. The presence of a spacer, therefore, may represent a substantial interval of no recovery. If it was evident that an individual piece had not rotated about a horizontal axis during drilling, an arrow was added to the label pointing to the top of the section. Azimuthal orientation of the core was not possible due to the free rotation of samples about a vertical axis within the core liner, although the fragments of each piece were marked and cut with a consistent orientation. After the vertical core orientation was noted, the pieces were split with a diamond saw into archive and working halves.

Each lithologic unit of the working half of the core was sampled (where recovery permitted) for shipboard measurement of physical properties, magnetic studies, X-ray fluorescence (XRF), and thin-section studies. Magnetic susceptibility was measured on the whole cores prior to splitting. The archive-half was described on the visual core description (VCD) form and was photographed before storage.

Visual Core Descriptions

Visual core description (VCD) forms for igneous and metamorphic rocks were used in the documentation of the igneous or metamorphic rock cores (see Site Summary appendices for each site chapter). The left column on the igneous and metamorphic core description form is a graphic representation of the rock pieces that compose the archive-half. A horizontal line across the entire width of the column denotes a plastic spacer. Vertically oriented pieces are indicated on the form by an upward-pointing arrow to the right of the piece. Shipboard samples and studies are indicated in the column headed "shipboard studies," using the following notation: XRD = (X-ray diffraction analysis); XRF = (X-ray

Table 1. Shipboard pore-fluid analytical methods.

Analysis	Technique	Units
Salinity	Goldberg refractometer	Unitless
Alkalinity	Gran titration	Millimolar (mM)
pH	TRIS-BIS buffers	pmH*
Chlorinity	Mohr titration	Millimolar (mM)
Potassium	Atomic emission spectrometry	Millimolar (mM)
Sodium	Atomic emission spectrometry	Millimolar (mM)
Lithium	Atomic emission spectrometry	Micromolar (μ M)
Calcium	EGTA titration	Millimolar (mM)
Magnesium	EDTA titration	Millimolar (mM)
Strontium	Atomic absorption spectrometry	Micromolar (μ M)
Ammonia	Colorimetry	Micromolar (μ M)
Silica	Colorimetry	Micromolar (μ M)
Boron	Colorimetry	Micromolar (μ M)
Fluoride	Ion-specific electrode	Micromolar (μ M)
Sulfate	Ion chromatography/turbidimetry	Millimolar (mM)

* See Gieskes et al. (1991).

fluorescence analysis); TS = (petrographic thin section); PP = (physical properties analysis); and PM = (paleomagnetic analysis).

To ensure consistent and complete descriptions, the visual core descriptions from the igneous and metamorphic rocks were entered into the computerized database HARVI. The database is divided into separate data sets for fine-grained rocks and coarse-grained rocks. Fine-grained rocks include all extrusions, and shallow intrusions which are aphyric or phenocrystic with a primarily glassy or cryptocrystalline matrix. Coarser-grained rocks include samples that are holocrystalline and whose groundmass minerals are visible in a 10× hand lens. Each record is checked by the database program for consistency and completeness, and is subsequently printed in a format that can be directly pasted onto the barrel sheet with the graphic representation of the core.

When describing sequences of rocks, the core was subdivided into lithologic units on the basis of changes in texture, grain size, mineral occurrence, and abundance, rock composition, and rock clast type. For each lithologic unit and section, the following information was recorded in the database system:

- A. The leg, site, hole, core number, core type, and section number.
- B. The unit number (consecutive downhole), position in the section, number of pieces of the same lithologic type, the rock name, and the identification of the describer.
- C. The Munsell color of the dry rock and the presence and general character of any structural fabric including deformation. Symbols for tectonic structures are provided in the explanatory notes for Lithostratigraphy and Sedimentology.
- D. The number of mineral phases visible with a hand lens and their distribution within the unit, together with the following information for each phase: (1) abundance (volume %); (2) size range in mm; (3) shape; (4) degree of alteration; and (5) further comments.
- E. The groundmass texture: glassy, fine grained (<1 mm), medium grained (1–5 mm), or coarse grained (>5 mm). Grain size changes within units were also noted.
- F. For igneous rocks the presence and characteristics of secondary minerals and alteration products.
- G. The abundance, distribution, size, shape, and infilling material of vesicles (including the proportion of vesicles that are filled by alteration minerals).
- H. For volcanic units: whether the flow is massive, pillowed, thin or sheetlike, brecciated, or a hyaloclastite.
- I. The relative amount of rock alteration, expressed both in the description and next to the graphic description of the archive-half. Rocks were classified as fresh (<2%); slightly altered (2%–10%); moderately altered (10%–40%); highly altered (40%–80%); very highly altered (80%–95%); and completely altered (95%–100%). These grades of alteration were expressed in columnar form as F, S, M, H, V, and C, respectively. The type, form, and distribution of alteration was also noted.
- J. The presence and location of veins, fractures, or other deformation features, including their abundance, width, mineral fillings or coatings, orientation, and associated wall rock alteration. The relationship of the alteration and vein-filling minerals with respect to veins and fractures was also noted. Vein networks and their mineralogy (if known) were indicated adjacent to the graphic representation of the archive-half.
- K. Other comments, including notes on the continuity of the unit within the core and on the interrelationship of units.

Basalt and diabase are termed aphyric (<1%), sparsely phyric (1%–2%), moderately phyric (2%–10%), or highly phyric (>10%), depending upon the proportion of phenocrysts visible with the hand lens or binocular microscope. Basalts are further classified by phe-

nocryst type (e.g., a moderately plagioclase-olivine phyric basalt contains 2%–10% phenocrysts, mostly plagioclase, with subordinate olivine). More specific rock names were given where chemical analyses or thin sections were available.

Lavas erupted on the seafloor typically show (a) a sparsely crystalline glassy margin overlying (b) a variolitic (synonymous with spherulitic) zone of quench phases, which may then grade into (c) a coarser microlitic zone toward the interior of the flow. In many samples, these zones are not well defined, and may be expressed as alternating layers or areas. Varioles commonly show a sheaflike or radial form, and microlites commonly show crystal clustering networks in areas of microlitic texture. The term intergranular refers to groundmass textures where individual crystals are granule-shaped with little intergrowth. Intersertal texture refers to granule-shaped crystals or glass that occupy interstices between unoriented feldspar laths.

Lavas intruded within the sedimentary pile may be characterized by baked or indurated sediment attached to glassy margins, both in intact flows or as random pieces. An abundance of glassy margins in a given section is taken to be indicative of a flow margin. Magmas intruded within sediments (either sills or dikes) may also appear as dismembered glassy flow breccias within a sediment host. The sediment will be contact metamorphosed at both the top and bottom contacts of a sill. Observation of contact relationships is especially important.

A breccia is defined as any rock composed of angular broken rock fragments held together by mineral cement or a fine-grained matrix. These can be volcanic or tectonic (fault breccia) in origin. Volcanic breccias are characterized by fragments of broken, but not crushed, basalt in a glassy, commonly altered, matrix. A fault breccia is characterized by fragments that are cataclastically deformed (crushed under brittle conditions) by movement along the fault. A cataclasite results from extensive dynamic metamorphism during which there is fracture and rotation of mineral grains or mineral aggregates, accompanied by extensive bending, breaking, and granulation of minerals.

Visual core descriptions of igneous rocks are given in the site summary appendices, and descriptions of each rock unit are available from the computerized database at the ODP repositories.

Thin-Section Descriptions

Thin sections of igneous rocks were examined to complement and refine the hand-specimen observations. The percentages and textural descriptions of individual phases were reported in the computerized database HRTHIN. The same terminology was used for thin-section descriptions as was used for the megascopic descriptions. Thin-section descriptions are included in the site summary appendices and are also available from the ODP computerized database. A table summarizing the thin section data is provided for each core.

X-Ray Fluorescence Analysis

Prior to analysis, samples were crushed in a Spex 8510 shatterbox using tungsten carbide or an agate mortar and pestle. Where recovery permitted, at least 20 cm³ of material was ground to ensure a representative sample. The tungsten carbide barrel introduces considerable tungsten contamination and minor Ta, Co, and Nb contamination, resulting in the powder becoming unsuitable for instrumental neutron activation (INNA) analysis. Niobium contamination resulting from grinding in the tungsten carbide barrel has been determined to be below 1 ppm (D. Sims, pers. comm., 1990).

A fully automated wavelength-dispersive ARL8420 XRF (3 kW) system equipped with an Rh target X-ray tube was used to determine the major oxide and trace-element abundances of whole-rock samples. Analyses of the major oxides were carried

out on lithium borate glass disks doped with lanthanum as a "heavy absorber" (Norrish and Hutton, 1969). The disks were prepared from 500 mg of rock powder that had been ignited for 3–4 hr at about 1025°C and mixed with 6.000 g of pre-weighed (on shore) dry flux consisting of 80% lithium tetraborate and 20% La₂O₃. This mixture was then melted in air at 1150°C in a Pt-Au crucible for about 10 min and poured into a Pt-Au mold using a Claisse Fluxer. The 12:1 flux-to-sample ratio and the use of the lanthanum absorber made matrix effects insignificant over the normal range of igneous rock compositions. Hence the relationship between X-ray intensity and concentration becomes linear and can be described by:

$$C_i = (I_i m_i) - b_i$$

where C_i = concentration of element i (wt%); I_i = peak X-ray intensity of element i ; m_i = slope of calibration curve for element i (wt %/cps); and b_i = apparent background concentration for element i (wt%).

The slope m_i was calculated from a calibration curve derived from the measurement of well-analyzed reference rocks (BEN, BR, DRN, from Geostandards, France; BHVO-1, AGV-1, from the U.S. Geological Survey; JGB-1, JP-1, from the Geological Survey of Japan; AII-92-29-1, from Woods Hole Oceanographic Institution/Massachusetts Institute of Technology; and K1919, from Lamont-Doherty Geological Observatory). The analyses of these standards derived from the calibration curves used are given in Table 2. The background b_i was determined by regression analysis from the calibration curves.

Systematic errors resulting from short-term or long-term fluctuations in X-ray tube intensity and instrument temperature were addressed by counting an internal standard between no more than six unknowns in any given run. The intensities of this standard were normalized to its known values, providing correction factors to the measured intensities of the unknowns. To check for errors, two glass disks were prepared for each sample. Accurate weighing

was difficult on board the moving platform of the *JOIDES Resolution* and was performed with particular care as weighing errors could be a major source of imprecision in the final analysis. Weights within 0.5 mg ($\pm 0.1\%$) were considered acceptable. Five weight measurements were taken for each sample and the average used as the true weight. Loss on ignition was determined by drying the sample at 110°C for 8 hr, and then by weighing before and after ignition at 1025°C in air.

Trace-element determinations were made on pressed-powder pellets prepared by pressing (with 8 Mpa of pressure) a mixture of 5.0 g of dry rock powder (dried at 110°C for >2 hr) and 30 drops of polyvinyl alcohol binder into an aluminum cap. A modified Compton scattering technique based on the intensity of the Rh Compton peak was used for matrix absorption corrections (Reynolds, 1967).

Replicate analyses of rock standards show that the major-element data are precise within 0.5% to 2.5%, and are considered accurate to 1% for Si, Ti, Fe, Ca, and K, and between 3% and 5% for Al, Mn, Na, and P. The trace-element data are considered accurate to between 2 and 3% or 1 ppm (whichever is greater) for Rb, Sr, Y, and Zr, and between 5% and 10% or 1 ppm for the others. The accuracy of Ba and Ce is considerably less, and they are reported primarily for purposes of internal comparison. Precision is within 3% for Ni, Cr, and V at concentrations >100 ppm, but 10% to 25% at concentrations <100 ppm. Analytical conditions for the XRF analyses are given in Table 3.

PHYSICAL PROPERTIES

Introduction

Shipboard determinations of physical properties are the basis for geotechnical stratigraphic studies and provide an important link connecting seismic geophysical records, electrical downhole logging data, and visual geological observations on recovered cores. The combination of these data sets provides an integrated view of the lithology and rock fabric of the section penetrated at the borehole. The function of the physical properties program during Leg 141 was to quantify downsection changes in the physical conditions and attributes of the rock and sediment of the south central Chile margin. It was anticipated that these properties would in part reflect the margin's unusual tectonic environment—the collision or along-trench subduction of an active spreading center. The study effort was therefore concerned in particular with identifying changes in physical state reflective of the special tectonic and thermal setting of the collision zone.

General

Physical properties (PP) regularly measured aboard the *JOIDES Resolution* are (1) index properties, (2) compressional (P -wave or V_p) sonic velocity, (3) thermal conductivity and, (4) undrained sediment shear strength. On Leg 141, sediment strength was not measured as vane-shear equipment was unavailable.

Index properties are the wet- and dry-bulk density, water content (wet and dry), grain density, wet and dry porosity, and void ratio attributes of recovered sediment and rock samples. At regular or selected core intervals, index properties were determined through gravimetric and volumetric techniques. A separate measure of "bulk density" was provided by the gamma-ray attenuation porosity evaluator (GRAPE) sensor, which is an integral part of the multi-sensor track system (MST). The MST scans the running length of recovered, whole-round cores.

Compressional-wave velocity (V_p) is the speed of propagation of compressional sound waves in sediment or rock. V_p was measured in the horizontal direction (i.e., normal to the long axis of the cores) by the continuous P -wave logger (PWL) of the MST system. Alternatively, at selected core positions, V_p was deter-

Table 2. Analyses of standard derived from the calibrations used for whole-rock analysis.

Run	Major trace precision standard						
	K1919 Z	K1919 DD	K1919 BB	K1919 CC	K1919 GG	K1919 FF	K1919 EE
Na ₂ O	2.39	2.35	2.29	2.32	2.36	2.39	2.33
MgO	6.73	6.75	6.79	6.79	6.78	6.73	6.76
MnO	0.17	0.17	0.17	0.17	0.17	0.17	0.17
TiO ₂	2.68	2.68	2.68	2.68	2.70	2.68	2.69
K ₂ O	0.54	0.54	0.54	0.54	0.54	0.54	0.54
SiO ₂	50.05	50.11	49.97	49.99	50.17	49.95	50.02
CaO	11.49	11.49	11.52	11.52	11.50	11.51	11.51
Fe ₂ O ₃	12.25	12.27	12.23	12.28	12.25	12.22	12.24
Al ₂ O ₃	13.76	13.72	13.71	13.73	13.67	13.69	13.69
P ₂ O ₅	0.28	0.28	0.28	0.28	0.27	0.28	0.28
Total	100.34	100.36	100.18	100.30	100.41	100.16	100.23

Run	Trace precision standard			
	BMO AA	BMO T	BMO V	BMO X
Nb	19	18	19	18
Zr	176	176	176	176
Y	26	26	25	25
Sr	392	392	392	392
Rb	9	9	9	10
Zn	101	102	104	99
Cu	141	140	141	142
Ni	118	118	118	119
Cr	283	289	283	283
V	333	328	336	330
TiO ₂	2.77	2.77	2.76	2.79
Ce	31	37	36	31
Ba	141	140	128	138

Table 3. X-ray fluorescence analytical conditions.

Element	Line	Crystal	Detector	Collimator	Peak angle (deg)	Background offset (deg)	Total count time (s)	
							Peak	Background
SiO ₂	K α	PET(002)	FPC	Coarse	109.06	0	40	0
TiO ₂	K α	LiF(200)	FPC	Fine	86.17	0	100	0
Al ₂ O ₃	K α	PET(002)	FPC	Coarse	144.52	0	100	0
Fe ₂ O ₃ *	K α	LiF(200)	FPC	Fine	57.53	0	40	0
MnO	K α	LiF(200)	FPC	Fine	63.04	0	40	0
MgO	K α	TLAP	FPC	Coarse	44.77	± 0.80	200	400
CaO	K α	LiF(200)	FPC	Coarse	113.14	0	40	0
Na ₂ O	K α	TLAP	FPC	Coarse	54.63	1.20	200	200
K ₂ O	K α	LiF(200)	FPC	Coarse	136.62	0	100	0
P ₂ O ₅	K α	Ge(111)	FPC	Coarse	140.96	0	100	0
Rh	K-C	LiF(200)	Scint	Fine	18.54	0	60	0
Nb	K α	LiF(200)	Scint	Fine	21.36	± 0.35	200	200
Zr	K α	LiF(200)	Scint	Fine	22.51	± 0.35	100	100
Y	K α	LiF(200)	Scint	Fine		± 0.40	100	100
Sr	K α	LiF(200)	Scint	Fine	25.07	± 0.41	100	100
Rb	K α	LiF(200)	Scint	Fine	26.57	± 0.60	100	100
Zn	K α	LiF(200)	Scint	Coarse	41.72	± 0.40	100	100
Cu	K α	LiF(200)	Scint	Coarse	44.94	± 0.40	100	100
Ni	K α	LiF(200)	Scint	Coarse	48.61	± 0.60	100	100
Cr	K α	LiF(200)	FPC	Fine	69.31	± 0.50	100	100
Fe	K α	LiF(220)	FPC	Fine	85.67	$-0.40+0.70$	40	40
V	K α	LiF(220)	FPC	Fine	123.13	-0.50	100	60
TiO ₂	K α	LiF(200)	FPC	Fine	86.10	± 0.50	100	40
Ce	L α	LiF(220)	FPC	Coarse	128.31	± 1.50	100	100
Ba	L β	LiF(220)	FPC	Coarse	128.89	± 1.50	100	100

*Total Fe as Fe₂O₃. FPC: Flow proportional counter using P₁₀ gas; Scint: NaI scintillation counter; Elements analyzed under vacuum using both goniometers at generator settings of 60 kV and 50 mA.

mined by the speed of transmission through isolated samples of unconsolidated material via the digital sediment core sound velocimeter (DSV) or, for more consolidated sediment and rock, the Hamilton Frame apparatus.

Thermal conductivity is the measure of the rate at which heat can be transferred by molecular conduction through a medium. Conductivity (k) is the coefficient that determines the rate of heat movement (Q) across a given or fixed temperature gradient (dT) established across a measured distance (dx), thus $Q = k (dT/dx)$. Thermal conductivity was determined at discrete core levels via the Thermcon-85 system.

The MST system also measured magnetic susceptibility at 10-cm positions on whole-round cores. This information is presented in sections treating paleomagnetic results (see Paleomagnetism section, this chapter).

With respect to the integrity of core sediment and rock samples, physical property measurements can be grouped into nondestructive and destructive types. Nondestructive measurements—bulk density, V_p , thermal conductivity—are performed on whole cores with the MST apparatus. DSV measurements of V_p can be carried out on half-round or split cores with little disturbance to the sediment column. Destructive measurements comprise all of the index properties and, for the most part, Hamilton Frame V_p runs. Acquiring these data requires the removal of discrete samples from the working half of split cores. Samples representative of the core were taken with regular intervals in sections of least disturbed material. Sample selection and spacing depended on the rate of core recovery, the type of measurement desired (see below), the thickness and homogeneity of the recovered sequence, and the degree of core disturbance caused by drilling and core-recovery procedures.

Index Properties

Methods

Bulk density was initially measured (or attempted) using the GRAPE on whole-round cores recovered by the advanced piston (APC), extended (XCB), and rotary (RCB) coring techniques. The GRAPE performs nondestructive and continuous measurements

of wet-bulk density by comparing the attenuation of gamma rays passing through the core with that through an aluminum standard (Boyce, 1976).

After collection, cores were cut into 1.5-m-long (or shorter) sections and allowed to reach laboratory temperature (3–4 hr) prior to being placed horizontally on a conveyor belt (track) and transported past GRAPE, PWL, and magnetic susceptibility sensors. The attenuation of gamma rays passing through the liner and core was measured every 2 to 5 cm, and bulk density was calculated from the attenuation values. GRAPE data were muted or filtered to remove readings made spurious by gas, gaps in the section, or endcap effects, then plotted. The GRAPE was calibrated with an aluminum standard once every 24 hr. Useful GRAPE data were, in general, only acquired from APC cores. Although XCB and RCB cores were routinely passed through the MST sensors, few accurate GRAPE values were collected from these commonly disturbed to disrupted core samples. All bulk density data are reported in units of either Mg/m³ or g/cm³, which are numerically equivalent values.

Destructive index properties were determined on discrete samples approximately 5 to 15 cm³ in volume in general accordance with the procedures outlined in ASTM (1989). Attempts were made to measure discrete index properties in a routine way, typically at the 100-cm interval of core sections, but the actual sampling point for routine measurements was dictated by the location of coherent material. On highly disturbed cores of fine-grained, weakly-consolidated sediment, virtually the only reason for collecting samples was for the systematic determination of grain density. However, for indurated material sufficiently coherent to shatter into small chunks and pieces, representative fragments were collected for the determination of a full suite of index properties. Additional core samples were taken to characterize changes in lithology and sediment strength. In general, an effort was made to collect thermal conductivity, index, and non-MST V_p values at the same or immediately adjacent intervals.

Samples collected for index properties were placed in small aluminum beakers and weighed, with a precision of 0.02 g, using two calibrated Scientech 202 electronic balances. The balance

was calibrated prior to service; a counterbalance weight within 5 g of the sample weight was used. Samples were oven dried at $110 \pm 5^\circ\text{C}$ for 24 hr (ASTM, 1989). Wet and dry volumes were measured using a Quantochrome helium penta-pycnometer. Weight and volume were determined within the prescribed precision of ± 0.02 g and ± 0.02 cm³. Representative sample-beaker weights and volumes were checked during the transit to the first site; good correspondence was noted between measured values and those listed in tables. Dry samples were routinely selected for powdering for the purpose of establishing that the volume of the coherent dried sediment did not differ significantly from that of a comminuted sample. It was determined that the volume of powdered sediment samples was effectively equivalent (± 0.02 g/cm³) to that of the dessicated coherent sediment contained in the calibrated beaker (see Physical Properties section, Site 859 chapter). Salinity-corrected physical properties were computed (via spreadsheet macros) for all samples assuming a pore-water salinity of 35‰.

Index property elements were entered into the ODP database. Derived property values were calculated by an Excel spreadsheet. Equations used are described by Lambe and Whitman (1979), Noorany (1984), and Taira et al. (1991).

The term "bulk density" refers to wet-sample or wet-bulk density and "porosity" refers to wet-porosity, and "water content" refers to the percentage of water in a wet sample released by means of 24 hr drying in an oven. Oven-dried samples were archived for other uses rather than cycled to the chemistry laboratory for routine carbonate analyses. Separate samples, in general collected immediately adjacent to index-property samples, were freeze-dried for routine determination of carbonate content. Unless otherwise noted, all discussions of Leg 141 index physical properties focus on wet density, wet-water content, and wet-porosity values, which are most representative of in-situ conditions. However, to assist mass-balance and mass-rate calculations, dry weight based index values, including void ratios, are tabulated for nearly all core samples.

Sonic Velocity

Methods

As noted, sonic velocity in recovered core was measured using three different techniques. The PWL of the MST apparatus continuously scans whole 1.5-m-long (or shorter) sections of undisturbed or little-disturbed APC/XCB cores. Scanning is at right angles to core length, and thus commonly in a direction parallel or subparallel to bedding. Logging is effected by transmitting a 500-kHz compressional wave pulse at a repetition rate of 1 kHz between two transducers. Both signal and receiving transducers are aligned perpendicular to the core axis. Their separation across the width of the core is automatically registered and entered into computer-based calculations that compensate for the thickness and velocity of the plastic core liner. Seawater was sprayed on the liner to improve acoustic coupling with the transducers. Discrete measurements were set for either a 2- or 5-cm interval and calibrated against a seawater standard at least once per drill site. As is true of the GRAPE measurements, generally only undisturbed advanced piston cores (APC) allowed the collection of useful PWL data. In general, XCB and RCB cores failed to completely fill the core liner, the separating air gap thus rendering the PWL ineffective. PWL data were edited and filtered to remove data that reflect gas, gaps, or endcap effects. Weak returns with signal strengths below a threshold value of 100 signal strength units were also removed. All velocity data are reported in units of either kilometers or meters per second.

The nondestructive DSV device measures V_p by transmitting a sound pulse between two piezoelectric transducers inserted into

the exposed sediment of the working half of a split core. On Leg 141, only the longitudinal transducer probes were installed, thus only parallel-to-core-axis readings were determined. The transmitting and receiving transducers are separated at a fixed distance close to 7.0 cm. For calibration runs, the actual separation is measured with a digital readout caliper, with a precision of about 0.001 cm. Calibration of the DSV is also achieved by submerging the transducers in deionized water and comparing the transmission time at a known laboratory temperature to that calculated from standard velocity-temperature tables. The calculations and standardizations are performed automatically by a Compaq microcomputer. On Leg 141, the water-standard method was used to calibrate DSV velocity measurements in sediment of known temperature.

The DSV performed well only on water-saturated core sediment. In general, an effort was made to make routine DSV observations on the same sections (1 and 4) of suitable cores and at roughly the same depth interval (100 cm). Additional measurements were made at obvious lithologic breaks, or other notable changes. Unfortunately the occurrence of gas pockets and core-sediment cavities and separations commonly either made DSV measurement impossible or produced meaningless readings. Hamilton Frame V_p measurements performed no better on sediment samples whose fabric integrity had been seriously disrupted by expanding gas.

The Hamilton Frame velocimeter requires that a sediment sample be removed from the working half of the recovered core. Operationally, the Hamilton Frame velocimeter is similar to that of the PWL and DSV in that V_p is determined by measuring the traveltime of a sonic pulse between a transmitting and receiving transducer placed across a measured thickness of sediment or rock. Sample thickness is measured electronically by a caliper attached to the frame and read directly (in mm) on a Tektronix oscilloscope display. Transmission time is measured with a Tektronix DC 5010 counter/timer system. Hamilton Frame measurements were taken on discrete samples sufficiently competent to transmit adequate signal strength and too stiff to permit insertion of the DSV transducer blades. Attempts were made to collect Hamilton Frame V_p measurements at routine intervals. At many sites velocity determinations were frustrated by gaseous or disrupted sediment or by the recovery of relatively brittle sediment that would crack or crumble under the slight pressure required to couple the transducers to the sample. Cores recovered using a cone-type rotary bit (RCB) tended to severely fragment indurated or semiconsolidated sedimentary material, and the recovered pieces were commonly too small or fractured to use on the Hamilton Frame. On cores disrupted into more coherent biscuits of semiconsolidated material, representative pieces were selected for Hamilton Frame V_p measurements, as were samples of more lithified rock types. Commonly part of the sample removed from the cores for Hamilton Frame use was appropriated for the collection of index property values. Hamilton Frame samples, unless needed for further index properties measurements, were returned (properly oriented) to the working half of the split core.

Where possible, Hamilton Frame V_p was measured in the A (parallel to the axis of the core), B (parallel to the face of the split core or sample) and C (perpendicular to the cut core face) directions. Usually only the A-axis direction was determined. All relevant measurements were entered into a data recording template that automatically calculated the sonic velocity.

Thermal Conductivity

Methods

Thermal conductivity is calculated from the increase in temperature of a needle probe inserted into the sample and heated for

a period of time. The sampled temperatures are fitted to the equation:

$$T(t) = (q/4\pi k) \ln(t) + L(t),$$

where T = temperature in the probe (K),

q = heat input per unit length per unit time (W/ms),

k = apparent thermal conductivity (W/m·K),

t = elapsed time (s), and

$L(t)$ = correction for background temperature drift, linearities arising from instrumental errors, and unspecified experimental aberrations.

Before starting thermal conductivity (TC) measurements, the whole-round core was allowed to reach equilibrium with the ambient laboratory temperature (3–4 hr). Through small holes drilled in the plastic core liner, the probes were inserted into the sediment. Although as many as five probes could be operated simultaneously, typically only 2 to 3 probes were used on any particular run. A separate probe was routinely emplaced in a standard of known thermal conductivity (usually black rubber of TC = 0.54 W/m·K). Equilibrium was determined by computer monitoring of the thermal drift of the probes embedded in the core sections; the acceptable drift is less than 4×10^{-2} °C/min, although a low but consistent drift can be accounted for in the final calculations. In practice, efforts were made to establish an acceptable drift rate. Thus TC computations were rarely drift corrected.

The thermal conductivity techniques used were described by Von Herzen and Maxwell (1959) and updated by Vacquier (1985). Prior to beginning the collection of thermal conductivity (TC) data, all available probes for use on soft sediment (full-space probes) were calibrated against on-board standards. Half-space probes for use with lithified and basement rocks were not calibrated. Calibration of full-space probes involved experimentally determining slope and intercept constants describing the relation of the TC measured by each probe to the known TC of four standards. Each probe was cycled through each of the four standard materials, representing a range of TC values (black rubber = 0.54, red rubber = 0.96, fused silica = 1.38, and Macor = 1.61). For each probe, at least four thermal conductivity measurements were carried out in each standard. Thus a minimum of 16 data points were used to establish a least-squares linear calibration fit of the constants for each probe. Plots of these data points, including the regression line and equation, are shown on Figures 20, 21, and 22. The empirically determined constants were incorporated in the appropriate file (PROBES.DAT) prior to beginning measurements of the TC value of recovered sediment samples. Empirically determined constants for half-space probes agreed with existing calibration values for all four standards, within experimental error.

TC data are reported in units of W/m·K, and have an estimated error of 5% to 10%. Where adequate estimates can be made of down-hole temperature, TC data can be corrected for in-situ pressure and temperature. A pressure correction of +1% for each 1800 meters, and a thermal correction of +1% for each +20°C differential between laboratory (typically 22°C) and the estimated downhole temperature, is typically used (Ratcliffe, 1960). Owing to uncertainties in establishing the in-situ temperature of recovered core samples, and the common circumstance that drilling greatly disrupted their in-section fabric, no temperature or pressure corrections were made to the TC data reported in this volume.

Soft-Sediment Full-Space Thermal Conductivity

The probes were positioned where visual examination or MST data indicated sediment samples of uniform properties. Data were acquired using a Thermcon-85 unit interface to an IBM-PC com-

patible microcomputer. After the core had reached thermal stability, the inserted probes were checked for an acceptable level of drift, then heated and the temperature rise recorded during a time interval of 6 min. In sediment too stiff or brittle to allow easy penetration of the probes, small pilot holes were drilled into the core material prior to careful insertion of each probe. The probe was sealed with a thermal compound.

Lithified Sediment and Hard Rock Half-Space Thermal Conductivity

Half-space TC measurements (i.e., conductivity measured on the open or cut surface of rock specimens) were performed during Leg 141, in particular at Site 863, where the most consolidated sedimentary rock was recovered. Standard laboratory procedures were followed, but it was found particularly important to allow adequate time (1 hr) for the samples to reach thermal equilibrium in the half-space bath.

IN-SITU TEMPERATURES

Scientific Objectives

Measurements of temperature are of great significance to one of the primary objectives of Leg 141, characterizing the tectono-hydrogeologic environment of the Chile Triple Junction region. The thermal state of the sediments and subducting oceanic crust is strongly influenced by, and is thus a good indicator of, fluid flow in this setting. In combination, analyses of thermal and chemical gradients provide indications of fluid flow over a wide range of advective flow rate and transient conditions. Techniques used for in-situ pore-fluid sampling during Leg 141 are covered in the Fluid Geochemistry section, this chapter. Several borehole-temperature logging tools were also used during Leg 141; these are described in the Wireline Measurements section (this chapter).

Water-Sampling Temperature Probe (WSTP) Temperature Measurements

The WSTP is a hybrid of two other tools, the Uyeda temperature tool (Yokota et al., 1980) and the Barnes fluid sampler (Barnes, 1979) (Fig. 23). A second-generation WSTP became available during ODP Leg 110 with improved sampling capabilities and a stouter temperature probe (Barnes, 1988). A third version of this tool was introduced during Leg 139 in anticipation of encountering extremely high-temperature, corrosive fluids (Davis, Mottl, Fisher, et al., in press). The Leg 141 iteration of the WSTP is essentially the same as that used in Leg 139 and so does not have the pressure-sensing capabilities available with the previous generation.

The older version of the WSTP temperature tool had a thin, stainless-steel probe that was pushed ahead of the bit into the undisturbed sediments at the bottom of a hole. The second generation tool had a probe tip with a minimum diameter of 1.3 cm that extended 8.3 cm past a 5.1-cm diameter pore-fluid filter block. The new WSTP probe includes a temperature-probe tip which is slightly longer and wider overall, although it ends with the same diameter (Fig. 23). Because the filter assembly has been made longer to improve fluid sampling performance, but tool length has been kept constant, the new temperature probe extends just 3.5 cm past the end of the filter. The current WSTP tool has two thermistor circuits (modified during Leg 139) with partially overlapping ranges to cover a wide variety of temperatures. However, due to the failure of the two-channel data logger on Leg 141 we had to use the old Uyeda data logger to sample the lower-range thermocouple only. Fortunately, there was very little effect on the quality of the data.

In operation, the WSTP is mounted inside a core barrel and lowered down the drill pipe by wireline while the bit is held above

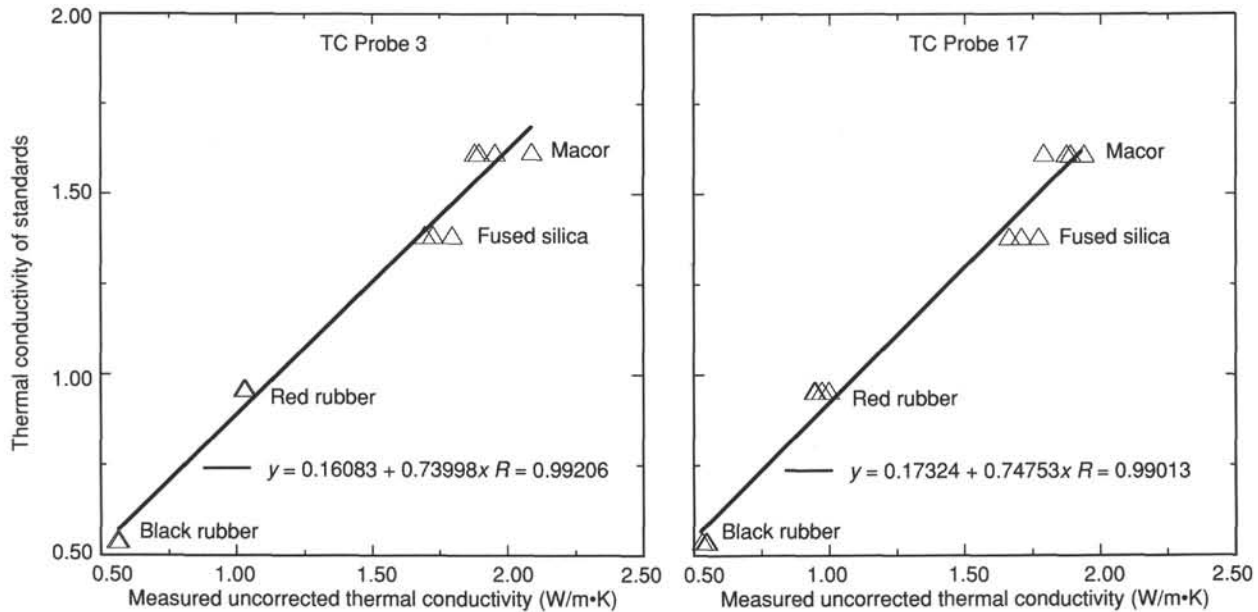


Figure 20. Thermal conductivity calibration data and corresponding linear regression equations for probes 3 and 17.

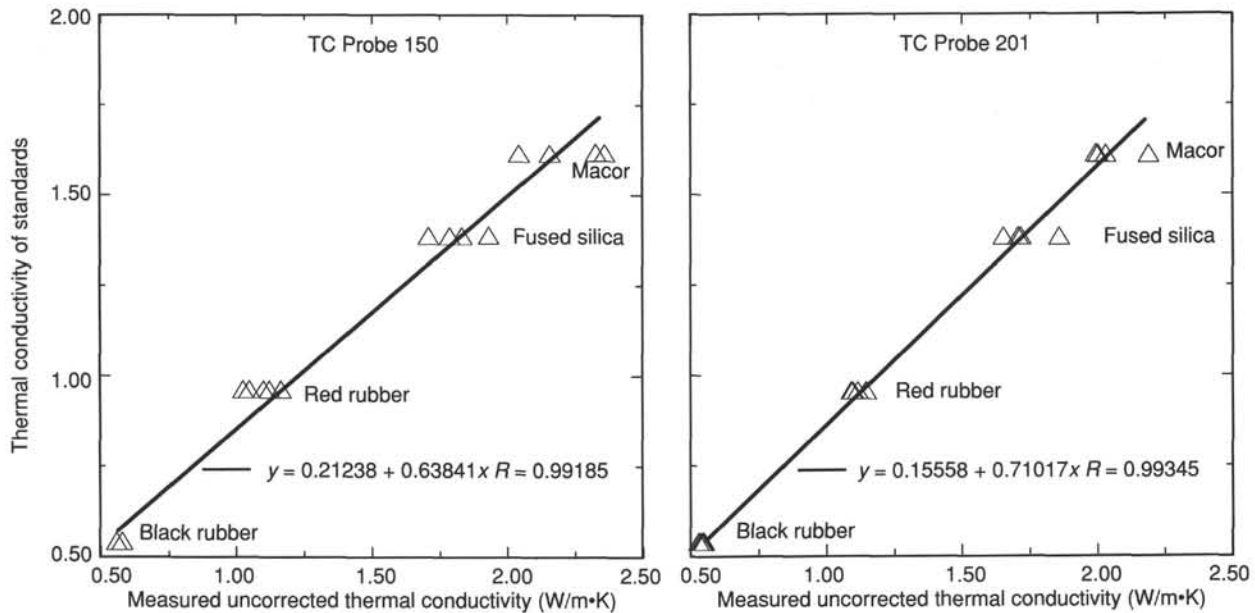


Figure 21. Thermal conductivity calibration data and corresponding linear regression equations for probes 150 and 201.

the bottom of the hole. The tool is held briefly above mudline to measure the temperature of bottom water. The tool is then lowered and latched into place, with the probe tip extending 1.1 m ahead of the bit. The drill string is lowered and the probe is forced into the bottom of the hole. A collected delivery system allows the probe to retract back up inside the bit should the formation prove to be too hard for penetration. With an APC/XCB BHA, the bit can be decoupled from the tool after penetration so that the probe will not be disturbed by drill string heave.

The driller can continue fluid circulation continuously during the station, if necessary, to keep the hole clear of fill, as circulation of cold bottom water in the hole will have little influence on measured temperatures at times less than a few hours after drilling, so long as the probe penetrates at least 50 cm (Fisher and Hounslow, 1990). Extrapolation to thermal equilibrium is re-

quired because insertion of the probe significantly disturbs formation temperatures and the instrument cannot be left in position to allow this disturbance to decay completely. Data reduction methods are described later in this section.

The relatively short length of the narrow probe commonly allows only 7–12 min of undisturbed measurements before a thermal disturbance is conducted down from the larger-diameter section above, limiting the accuracy of temperature extrapolations to about $\pm 0.1^{\circ}$ – 0.2° C. Because the exact depth of penetration of the tool is never known, all temperatures measured with the WSTP must be considered lower bounds on in-situ conditions. From the shape of the temperature-time records and comparison with nearby measurements it is often possible to determine if the tool was pressed into fill at the bottom of a hole or if the formation cracked upon insertion. A review of thermal data obtained with

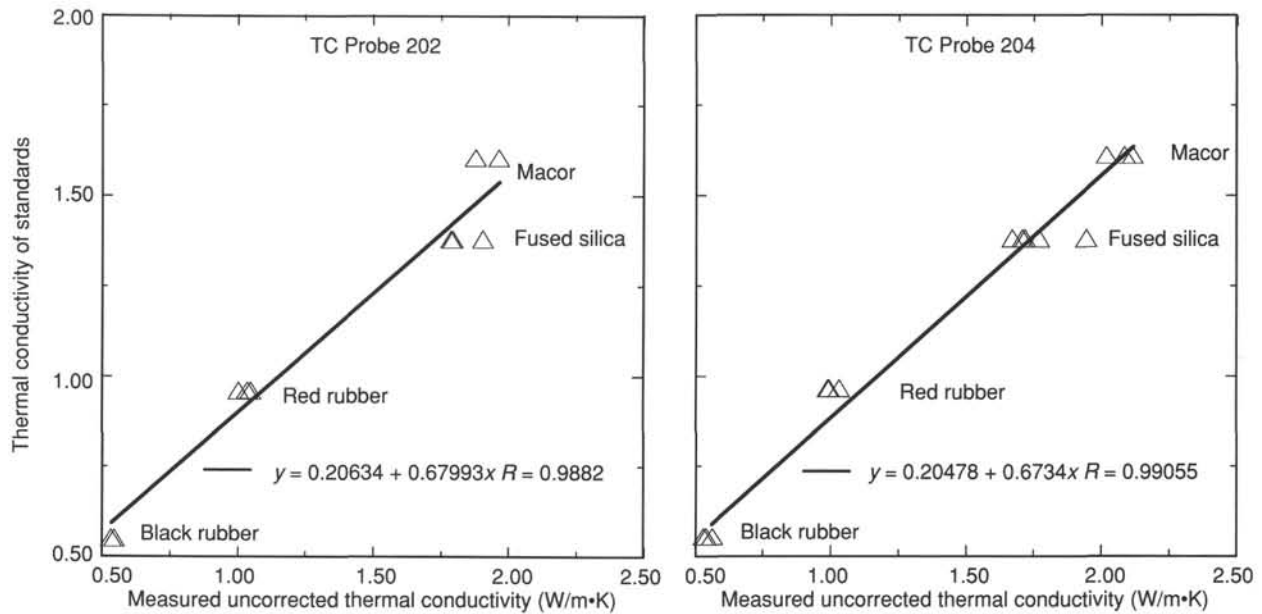


Figure 22. Thermal conductivity calibration data and corresponding linear regression equations for probes 202 and 204.

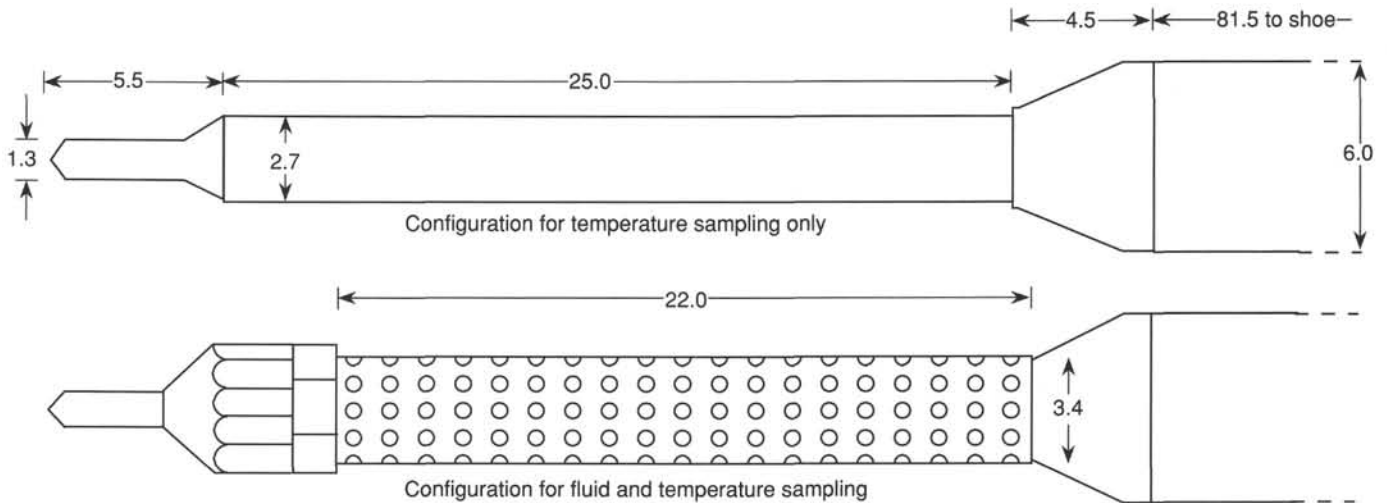


Figure 23. Scale cross-sections of the WSTP probe assembly, configured for temperature only, and for temperature and water sampling. All dimensions are in centimeters. The probe tips extend 1.1 m ahead of the bit when latched in place.

this type of probe during the DSDP is given by Hyndman et al. (1987).

APC-Tool Temperature Measurements: ADARA system

The new advanced piston core heat-flow coring shoe (ADARA tool) was also used during Leg 141. The ADARA tool is used for measuring in-situ sediment temperatures during regular piston-coring operations. The instrument is built into a cylindrical frame and contains an electronics section composed of three circuit boards and two battery packs. This frame fits inside an annular cavity in a special coring shoe. Two steel prongs extend from the base of the frame and anchor the electronics in place inside the shoe. Inside one of the two prongs is a platinum resistance-temperature device (RTD) that has been calibrated over a range of -20° to 100°C, with resolution of 0.01°C. The RTD prong is coated with thermally conductive grease to assure a good contact

with the wall of the cutting shoe. The instrument runs on standard camera batteries.

The ADARA tool is programmed after it has been inserted into the coring shoe, and repeated deployments can be run without removing the tool or batteries. The tool is run off a PC through an interface and contains a microprocessor and 32 kb of nonvolatile memory. The tool operating system is downloaded from the computer, and the user defines a table of events, which includes the measurement frequency and total time of operation. During Leg 141, data were generally collected at a 5-s time interval. Between individual measurements, and optionally for extended periods, the tool can be programmed to “sleep” to conserve power.

A crossover subassembly with o-rings seals the cavity containing the electronics after programming and starting the test sequence. The shoe is then placed at the front end of a core barrel and lowered down the pipe. The shoe is typically held just above

the mudline to measure the temperature of bottom water, then lowered into the bottom-hole assembly. The core barrel is deployed in the standard way, fired out through the bit using hydraulic pressure from the rig pumps, but it is left in place for 10 min instead of being retrieved immediately, so that the tool can begin thermal equilibration with the formation. After the core barrel is returned to the ship, the coring shoe is removed and the temperature data are uploaded to the PC for reduction.

We experienced considerable problems with the ADARA tool in rough sea conditions with repeated tool disturbance resulting in noisy, anomalous temperature records. The formations encountered on Leg 141 were also very well consolidated at shallow depths, limiting the depth of deployment of the tool in the hydraulic piston core shoe. For these two reasons, all too often we had to rely on just the WSTP data.

Data Reduction

Although the WSTP and ADARA tools have different geometries, the methods used for analysis of recovered temperature data are similar. For the WSTP, the thermal response of the cylindrical probe to a pulse of heating (or cooling) is given by Bullard (1954). The equivalent theory for the ADARA tool is discussed by Horai and Von Herzen (1985). For both instruments, synthetic-type curves are constructed, based on tool geometry, sampling interval, and the thermal properties of the tools and surrounding sediments. Both tools have thermal time constants of several minutes under normal conditions, requiring that the probes be kept in bottom for at least 10–15 min to allow extrapolation of the temperature curves with confidence.

The theoretical decay curves from the shipboard program APCTFIT (developed by K. Horai and K. Becker) simulate the instantaneous heating (or cooling) of the sediment following the ADARA probe penetration, but in practice a finite time is required for the sensors to reach a maximum temperature. As a result, the effective origin time of the thermal pulse is delayed as a function of tool and sediment properties. In addition, the recorders sample temperatures at fixed intervals, leaving the exact penetration time uncertain. An effective penetration time and an extrapolated temperature are estimated for the ADARA tool by shifting the time axis of the theoretical thermal decay curves to fit the actual data. Temperatures from approximately the first 5–10 measurements (20–50 s) following penetration commonly do not follow the theoretical curves, but later parts of the records usually provide a very good match. The choice of which data should be included in the matching, and which time shift should be used, is partly subjective; it is probably best to use as much of the decay curve as possible. The variations in extrapolated temperatures that result from choosing different time intervals and time shifts can be used to estimate errors associated with the temperatures finally assigned to represent in-situ conditions.

The WSTP tool temperatures were subject to similar problems related to tool response and uncertainty in the time of penetration, and commonly do not follow the theoretical response curves within the first few minutes of cooling. The thermal response of a cylindrical probe to a pulse of heating (or cooling) is given by the function $F(\alpha, \tau)$ described by Bullard (1954). This function approaches $1/t$ after several minutes, given the small diameter of the probe. Equilibrium temperatures for the WSTP data were determined by transforming the data into functions of $1/t$ so that linear trends that properly fell on theoretical decay curves of the later stages of cooling could be readily identified. Disturbances in the cooling trend due to cracking of the formation or propagation of heat through the tool into the formation could also be readily identified in $1/t$ space. Equilibrium temperature was determined as the temperature when the linear trend is extrapolated to a $1/t$ of zero.

WIRELINE MEASUREMENTS

Logging Tool Strings

Downhole logging directly determines physical and chemical properties of formations adjacent to the borehole. Interpretation of these continuous, in-situ measurements can yield a stratigraphic, lithologic, geophysical, and mineralogic characterization of the site. After coring is completed at a hole, a tool string is lowered downhole on a seven-conductor cable, and each of several tools in the tool string continuously monitors some property of the adjacent borehole. Three Schlumberger tool strings were used on Leg 141: the geophysical tool string (quad-combo), formation microscanner sonde (FMS), and geochemical combinations. The Lamont-Doherty temperature tool was attached to the base of the tool strings to obtain borehole temperatures for thermal gradient determinations. In addition, a vertical seismic profile (VSP) experiment was conducted with the Schlumberger Well Seismic Tool (WST).

The geophysical tool string combination used on Leg 141 consisted of long-spaced sonic (LSS), natural gamma-ray tool (NGT), neutron porosity tool (CNT-G), high-temperature lithodensity tool (HLDT), mechanical caliper (MCD), and phasor induction tool (DIT). This tool combination measures compressional wave velocity and provides indicators of the two variables that most often control velocity: porosity, as indicated by density or resistivity, and clay content, as indicated by the natural gamma-ray radiation. On occasion, the geophysical tool string was broken up into two tool strings consisting of the gamma ray, sonic, caliper, and resistivity on one string, and gamma ray, neutron porosity, and density on the other tool string (which is called the lithodensity tool string).

The FMS tool string included not only the FMS but also a general-purpose inclinometer tool (GPIT) that spatially orients the FMS resistivity image of the borehole wall. The tool string also contained a natural gamma-ray tool (NGT) to allow depth correlation of the FMS data with other logs.

The geochemical combination for Leg 141 consisted of the NGT, aluminum clay tool (ACT), and gamma spectrometry tool (GST). This tool combination measures the relative concentrations of silicon, calcium, iron, sulfur, hydrogen, chlorine, potassium, thorium, uranium, and aluminum.

Logging Tool Descriptions

A brief description of logging tools run during Leg 141 follows. A detailed description of logging tool principles and applications is provided in Schlumberger (1989), Serra (1984, 1989), and Timur and Toksoz (1985).

Electrical Resistivity (DIT)

The phasor induction tool provides three different measurements of electrical resistivity, each one with a different depth of investigation. Two induction devices (deep and medium resistivity) send high-frequency alternating currents through transmitter coils, creating magnetic fields that induce secondary (Foucault) currents in the formation (Fig. 24A). These ground-loop currents produce new inductive signals, proportional to the conductivity of the formation, which are recorded by the receiving coils. Measured conductivities then are converted to resistivity. A third device (spherically focused resistivity, Fig. 24B) measures the current necessary to maintain a constant voltage drop across a fixed interval. Vertical resolution is about 150 cm for the medium device, 200 cm for the deep resistivity device, and about 75 cm for the focused resistivity device.

Water content and salinity are by far the most important factors controlling the electrical resistivity of rocks. To a first order,

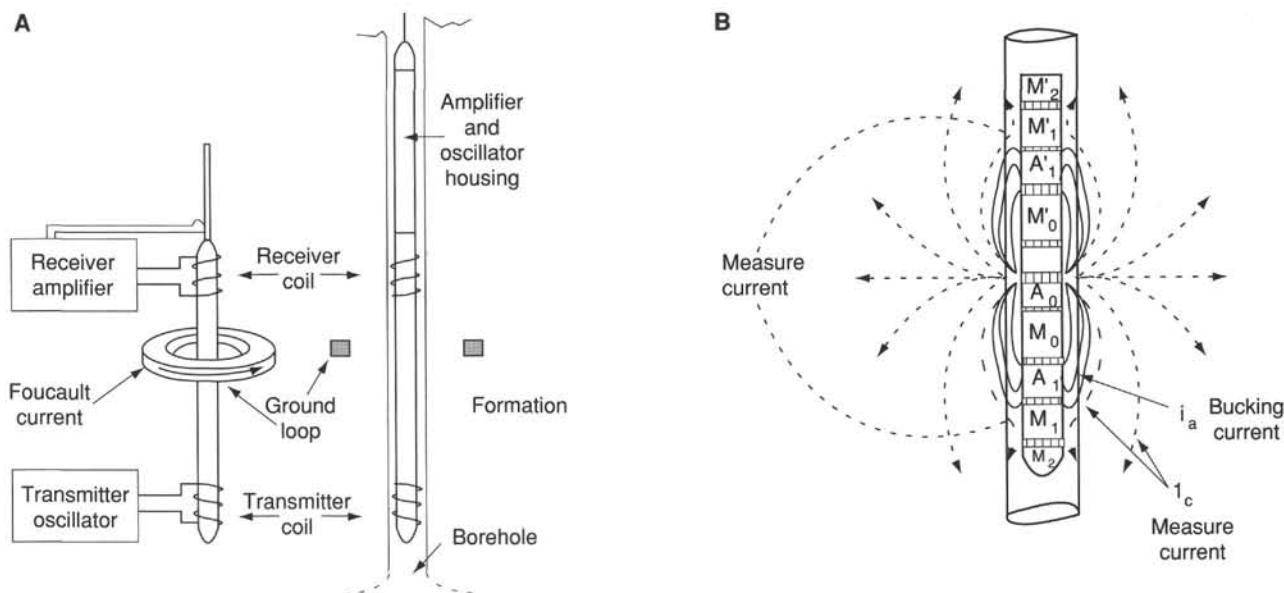


Figure 24. Sketch of the Schlumberger resistivity devices used in the Ocean Drilling Program: (A) phasor induction tool (DIT), and (B) spherically focused resistivity tool (SFLU).

resistivity varies as the inverse square root of porosity (Archie, 1942). Other factors influencing resistivity include the concentration of hydrous and metallic minerals, vesicularity, and geometry of interconnected pore space.

Sonic Velocity Measurements (LSS)

The long-spaced sonic tool uses two acoustic transmitters and two receivers to measure the time required for sound waves to travel over source-receiver distances of 2.4, 3.0, and 3.6 m (Fig. 25). The raw data are expressed as time required for a sound wave to travel through 0.31 m of formation; these traveltimes are then converted to sonic velocities. First arrivals for the individual source-receiver paths are used to calculate the velocities of the different waves traveling in the formation (compressional, shear, etc.). Only compressional-wave velocity is determined during data acquisition, but waveforms are recorded for post-cruise determination of shear-wave velocities and possibly improved compressional-wave velocities. The vertical resolution of the tool is 60 cm. Compressional-wave velocity is dominantly controlled by porosity and degree of lithification; a decrease in porosity or an increase in lithification will increase the velocity.

Mechanical Caliper Device (MCD)

The mechanical caliper device provides a measure of borehole diameter (up to 16 in. or 40.6 cm). The hole diameter log is used to detect washouts or constrictions. Borehole diameter significantly affects many of the other logging measurements, and the hole diameter is an important input to log correction routines. The caliper tool is subject to sticking when formation mud gets into its mechanical parts, resulting in bimodal (fully open or nearly fully closed) readings. In contrast, the measurement of hole diameter produced by the high-temperature lithodensity tool is much more reliable. Consequently, on Leg 141 the MCD tool was used primarily to provide centralization and associated improved log quality for the sonic log.

Natural Gamma-Ray Tool (NGT)

The natural gamma-ray tool measures the natural radioactivity of the formation. Natural gamma rays are most commonly emitted

by the radioactive isotope ^{40}K and by the radioactive elements of the U and Th series. Gamma rays emitted from the formation close to the borehole wall are measured by a scintillation detector mounted inside the tool. They are analyzed by dividing the incident gamma-ray spectrum into five discrete energy windows. The total counts recorded in each window, at each depth increment in the well, are analyzed to determine the elemental abundances of K, U, and Th. The final outputs are the total gamma ray (SGR), a uranium-free gamma-ray measurement (CGR), and the concentrations of potassium (POTA, wt% or decimal fraction), thorium (THOR, ppm), and uranium (URAN, ppm). The vertical resolution of the log is about 46 cm.

Because radioactive elements tend to be most abundant in clay minerals, the gamma-ray curve is commonly used to estimate the clay or shale content. There are formations, however, for which the radioactivity ranges from moderate to extremely high values as a result of the presence of volcanic ash, potassic feldspar, or other radioactive minerals.

Lithodensity Tool (HLDT)

The high-temperature lithodensity tool uses a ^{137}Cs gamma-ray source and measures the resulting flux at fixed distances from the source (Fig. 26A). Under normal operating conditions, attenuation of gamma-rays is caused mainly by Compton scattering (Dewen, 1983). Formation density is extrapolated from this energy flux by assuming that the atomic weight of most rock-forming elements is approximately twice the atomic number. A photoelectric effect index is also provided. Photoelectric absorption occurs in the energy window below 150 keV and depends on the energy of the incident gamma-ray, the atomic cross section, and the nature of the atom. Because this measurement is almost independent of porosity, it can be used directly as an indicator of matrix lithology. The radioactive source-and-detector array is placed in a tool that is pressed against the borehole wall by a strong bowspring arm; the position of this spring arm relative to the tool indicates hole diameter (up to 17.2 in. or 43.7 cm). Excessive roughness of the hole will cause some drilling fluid to infiltrate between the detector and the formation. As a consequence, density readings may be artificially low, but can be

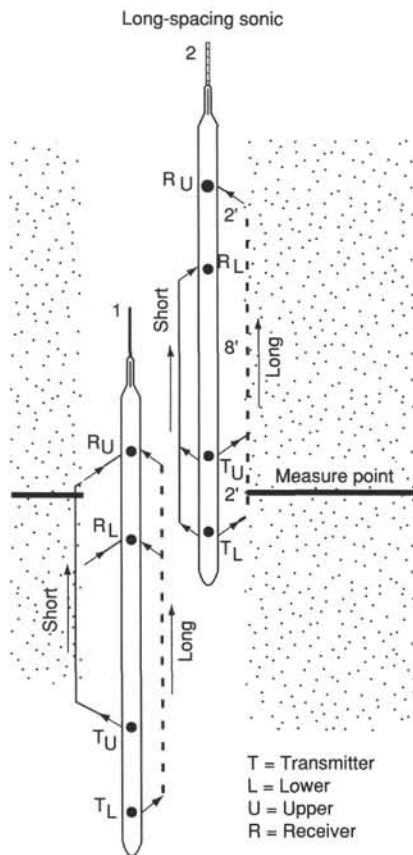


Figure 25. Sketch of the Schlumberger acoustic tool (Long Spacing Sonic; LSS).

corrected using caliper data. The vertical resolution is about 38 cm.

Compensated Neutron Porosity Tool (CNT-G)

A radioactive source mounted on the compensated neutron porosity tool emits high energy neutrons (4 MeV) into the formation, where they are scattered and slowed by collisions with other nuclei. When the neutrons reach a low energy level (0.025 MeV) they are captured and absorbed by atomic nuclei such as hydrogen, chlorine, silicon, and boron. The scattering cross-section is the quantity that describes the rate at which neutrons are slowed. Because the scattering cross-section for hydrogen is about 100 times larger than for any other common element in the crust, most energy dissipation is caused by collisions with water molecules. Therefore, a change in the number of neutrons detected at a receiver can be related to water content. In practice, an array of detectors is used to minimize borehole or drilling fluid effects (Fig. 26B). The device also measures the epithermal (intermediate energy) neutron flux, which is an indicator of free water only, expressed as epithermal neutron porosity. The neutron porosity is thus proportional to bound water (in clays, etc.) within the formation. The vertical resolution of the tool is about 46 cm.

Gamma Spectrometry Tool (GST)

The induced spectral gamma-ray tool consists of a pulsed source of 14-MeV neutrons and a gamma-ray scintillation detector. A shipboard computer performs spectral analysis of gamma rays generated by the interactions between neutrons emitted by the source and atomic nuclei in the formation (Hertzog, 1979). Characteristic sets of gamma rays from six elements dominate the spectrum, permitting calculation of six elemental yields: calcium,

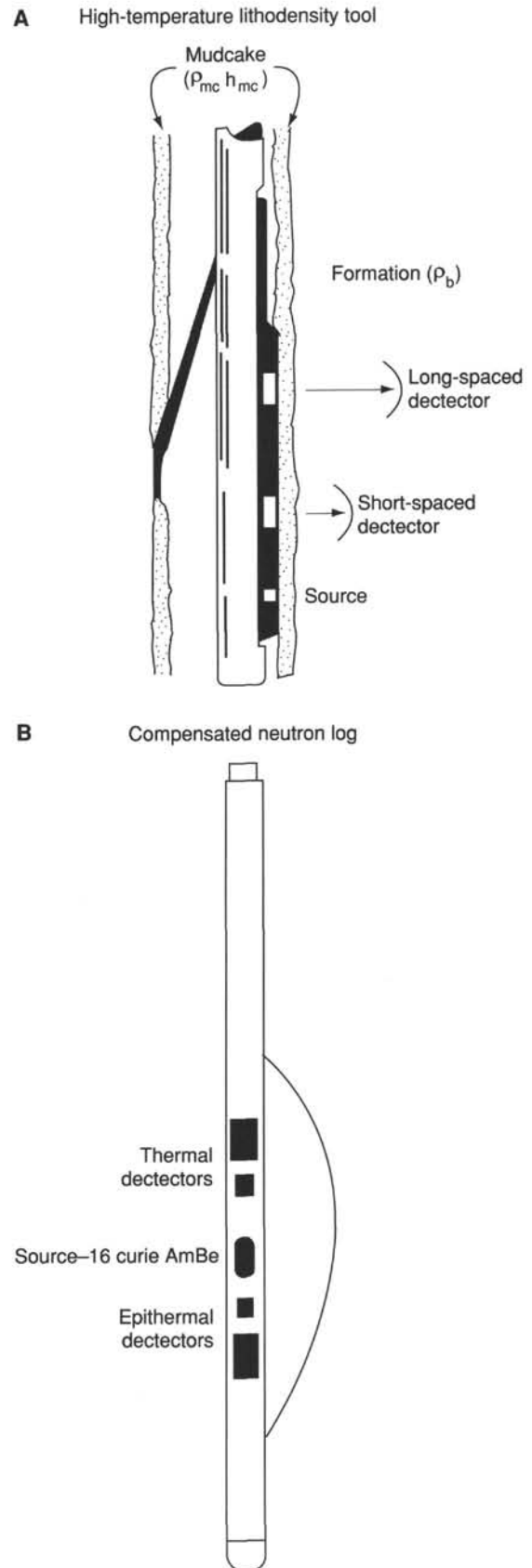


Figure 26. Schematic drawing of the (A) high-temperature density (HLDT) and (B) neutron porosity (CNT-G) tools used in the Ocean Drilling Program.

silicon, iron, chlorine, hydrogen, and sulfur. The tool normalizes their sum, so that the yields do not reflect the actual elemental composition. Instead, ratios of these elemental yields are commonly used in interpreting the lithology, porosity, and salinity of the formation fluid. Shore-based processing is used to compute new elemental yields and absolute dry weight fractions of the major oxides.

Aluminum Clay Tool (ACT)

Aluminum abundance is measured by the aluminum clay tool. It is determined by neutron-induced late gamma-ray spectrometry using californium as the chemical source. The decay of the nucleus emits characteristic gamma rays detected within a series of energy windows by the natural gamma tool. By placing NaI detectors (NGT tools) both above and below the neutron source, contributions from natural gamma-ray activity can be removed.

Calibration to elemental weight percent is performed by taking irradiated core samples of known volume and density and measuring their gamma-ray output while they are in a jig attached to the logging tool (generally after logging).

Formation Microscanner Sonde (FMS)

The FMS produces high-resolution microresistivity images of the borehole wall that can be used for detailed sedimentological or structural interpretations and for determining fracture and breakout orientations. The tool (Fig. 27) consists of sixteen electrodes (called buttons) on each of four orthogonal pads that are pressed against the borehole wall. The electrodes are spaced about 2.5 mm apart and are arranged in two diagonally offset rows of eight electrodes each. The focused current that flows from the buttons is recorded as a series of curves that reflect the microresistivity variations of the formation. On board or shore-based processing converts the measurements into complete, spatially oriented images of the borehole wall. Further processing can provide measurements of dip and direction or azimuth of planar features. The vertical resolution of the FMS is 1 cm, but coverage is restricted to about 22% of the borehole wall for each pass of the tool, assuming a hole diameter of 9.75 in. (24.7 cm).

Applications of the FMS images include detailed correlation of coring and logging depths, orientation of cores, mapping of fractures, faults, foliations, and formation structures, as well as determining strikes and dips of bedding. The FMS can also be used to measure stress in the borehole through breakout delineation. In an isotropic, linearly elastic rock subjected to an anisotropic stress field, breakouts form in the direction of the least principal horizontal stress. An important limitation of the tool is the restriction of hole diameter to less than 40.6 cm (16.0 in.). Thus, no useful information can be obtained from seriously washed-out hole sections.

General Purpose Inclinator Tool (GPIT)

This tool provides a measurement of borehole inclination, the orientation of the tool with respect to the earth's magnetic field using a three-component magnetometer, and tool motion using an accelerometer. It is run with the FMS to provide spatial orientation of the borehole wall images.

Lamont-Doherty Temperature Tool (TLT)

The LDGO temperature tool is a self-contained tool that can be attached to any Schlumberger tool string. Data from two thermistors and a pressure transducer are collected at a predetermined rate between 0.5 and 5.0 s and stored in a Tattletale computer within the tool. Following the logging run, data are dumped from the Tattletale to a shipboard computer for analysis. A fast-response, low-accuracy thermistor is able to detect sudden, very small temperature excursions caused by fluid flow from the

formation. A slow-response, higher accuracy thermistor can be used to estimate heat flow, provided the history of drilling-fluid circulation in the hole and at least two temperature logs are available (Jaeger, 1961). Data are recorded as a function of time; conversion to depth can be based on the pressure transducer or, preferably, on simultaneous recording by Schlumberger of both depth and time.

Other Downhole Measurements

Well Seismic Tool (WST)

The well seismic tool measures seismic velocities by recording the time required for a seismic signal to travel from a source deployed off the side of the ship to a sidewall clamped geophone (Fig. 28). During Leg 141, the tool was used to record a vertical seismic profile at Site 859. The source for the seismic signal was a 400-in.³ watergun.

The WST is clamped in the borehole at a series of depths, and at each the watergun is fired four times. The seismograms observed from each group of four shots are summed to improve the signal-to-noise ratio. The resulting vertical seismic profile is used to relate seismic reflection events to observations in the borehole, specifically core and log data. The traveltime of a direct arrival in the vertical seismic profile is the one-way vertical traveltime from the surface to a known depth in the borehole. This may be doubled to determine the two-way vertical traveltime to that depth. The full seismograms of the vertical seismic profile can be used to identify the travel paths of events in the seismic reflection record, to look ahead of the drill bit as reflection events are approached, and to verify that seismic reflection events of interest have actually been penetrated.

Log Data Quality

The quality of log data may be seriously degraded in sections of the borehole with very large diameter or with rapid changes in the hole diameter. Resistivity and velocity measurements are less sensitive to borehole size variation, whereas the nuclear measurements (density, neutron porosity, and both natural and induced spectral gamma-ray) are more seriously impaired because of the large attenuation by the borehole fluid. Corrections can be applied to the original data to reduce the effects of these conditions.

Logs from different tool strings may have small depth mismatches, caused by either cable stretch or ship heave during recording. Small errors in depth matching can impair the results in zones of rapidly varying lithology. To minimize the effects of ship motion, a hydraulic heave compensator adjusts for rig motion during logging operations.

Log Analysis

During logging, incoming data are observed on a monitor oscilloscope and simultaneously recorded on digital tape in the Schlumberger logging unit. After logging, the Schlumberger tapes are read by computer in the downhole measurements laboratory and reformatted to a file format compatible with the Teralog log-interpretation software package. Most log interpretation (except geochemical log analysis) is carried out aboard ship; further analysis and interpretation are undertaken after the cruise at the Borehole Research Laboratory of Lamont-Doherty Geological Observatory.

Synthetic Seismograms

Synthetic seismograms are generated from velocity data obtained with the long-spaced sonic (LSS) tool, and either the bulk density data from the lithodensity tool, or a pseudodensity log calculated from other log data. In many cases, a simple constant density can be assumed. Experience shows that this often gives surprisingly good results, because both velocity and density usu-

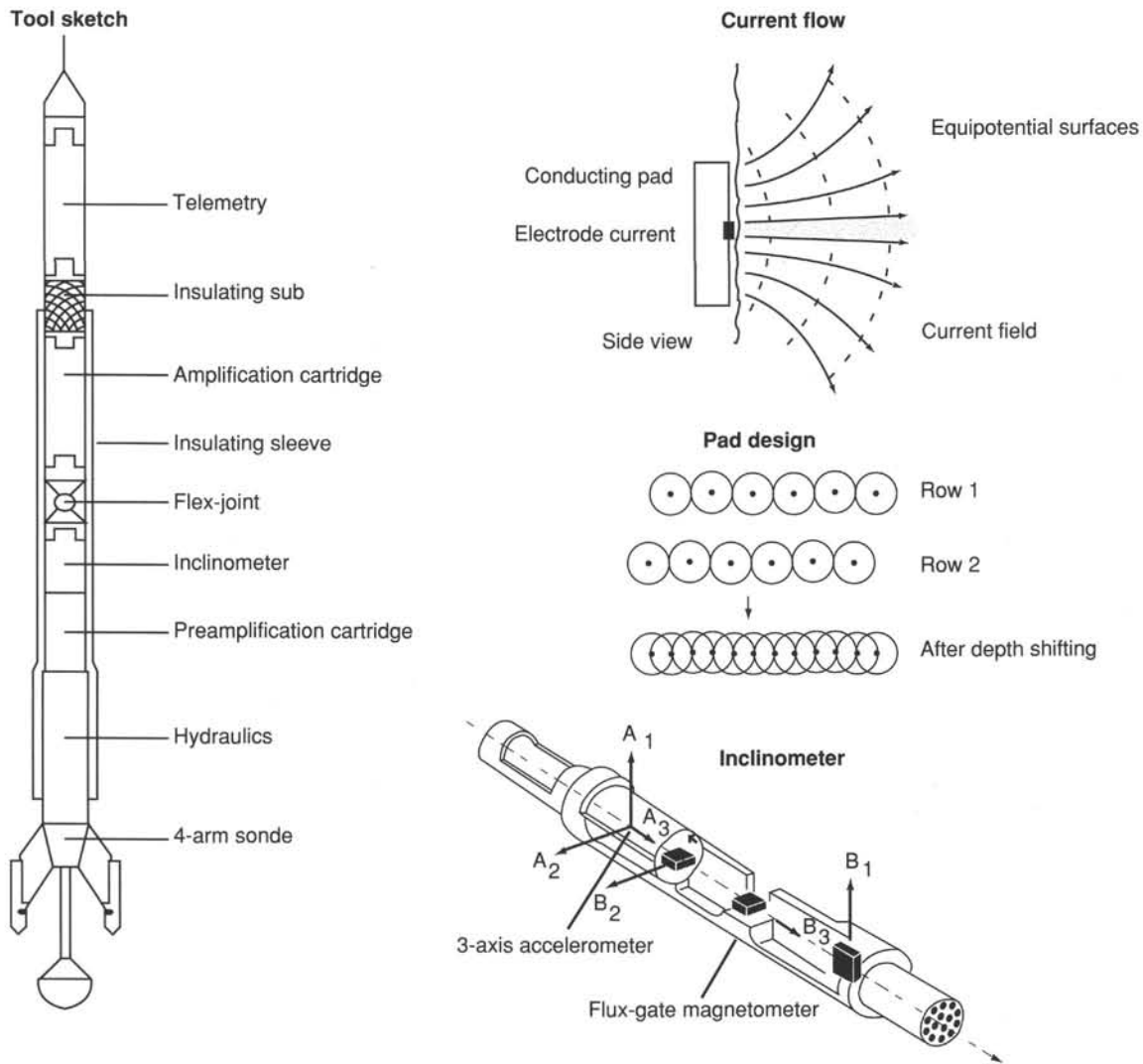


Figure 27. Sketch of the four-pad formation microscanner sonde (FMS), pad configuration, and inclinometer used for FMS image orientation and speed correction.

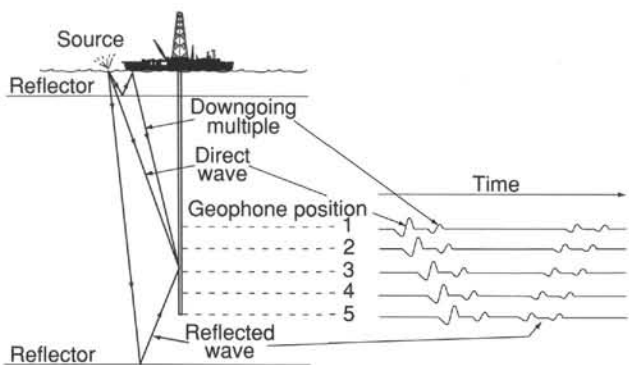


Figure 28. Use of a sidewall-clamped geophone located at different depths in the wellbore. The Schlumberger well seismic tool (WST) records the arrivals of an acoustic wave generated by a seismic source hung from the side of the ship.

ally respond similarly to changes in porosity. When velocity and density are highly correlated, synthetic seismograms using either constant density or an actual density log are virtually identical.

The velocity and density logs are used in a program that generates an impedance log (velocity \times density) that is convolved with a zero-phase Ricker or other assumed wavelet. The frequency of this wavelet can be varied to be consistent with the source used to generate the original seismic profile. A 30-Hz wavelet is capable of a vertical resolution on the order of 30 m, so reflectors cannot generally be attributed to smaller-scale lithologic intervals.

REFERENCES

Archie, G.E., 1942. The electrical resistivity log as an aid in determining some reservoir characteristics. *J. Pet. Tech.*, 5:1-8.
 ASTM (American Society of Testing and Materials), 1989. *Annual Book of ASTM Standards for Soil and Rock; Building Stones: Geotextiles* (Vol. 04.08): Philadelphia (ASTM), 168-862.
 Barnes, R.O., 1979. Operation of the IPOD in-situ pore water sampler. In Sibuet, J.-C., Ryan, W.B.F., et al., *Init. Repts. DSDP*, 47 (Pt. 2): Washington (U.S. Govt. Printing Office), 19-22.
 _____, 1988. ODP in situ fluid sampling and temperature measurement: a new wireline tool. In Masche, A., Moore, J.C., et al., *Proc.*

- ODP, *Init. Repts.*, 110: College Station, TX (Ocean Drilling Program), 55–63.
- Barron, J.A., 1985. Miocene to Holocene planktic diatoms. In Bolli, H.M., Saunders, J.B., and Perch-Nielsen, K. (Eds.), *Plankton Stratigraphy*: Cambridge (Cambridge Univ. Press), 763–809.
- Barron, J.A., Keller, G., and Dunn, D.A., 1985. A multiple microfossil biochronology for the Miocene. In Kennett, J.P. (Ed.), *The Miocene Ocean: Paleooceanography and Biogeography*. Mem.—Geol. Soc. Am., 163:21–36.
- Barron, J.A., Nigrini, C.A., Pujos, A., Saito, T., Theyer, F., Thomas, E., and Weinreich, N., 1985. Synthesis of biostratigraphy, central equatorial Pacific, Deep Sea Drilling Project Leg 85: refinement of Oligocene to Quaternary biochronology. In Mayer, L., Theyer, F., Thomas, E., et al., *Init. Repts. DSDP*, 85: Washington (U.S. Govt. Printing Office), 905–934.
- Bé, A.W.H., and Tolderlund, D.S., 1971. Distribution and ecology of living planktonic Foraminifera in surface waters of the Atlantic and Indian Oceans. In Funnell, B.M., and Riedel, W.R. (Ed.), *The Micropaleontology of Oceans*: Cambridge (Cambridge Univ. Press), 105–149.
- Berggren, W.A., Kent, D.V., Flynn, J.J., and van Couvering, J.A., 1985. Cenozoic Geochronology. *Geol. Soc. Am. Bull.*, 96:1407–1418.
- Biscaye, P.E., 1964. Mineralogy and sedimentation of the deep-sea sediment fine fraction in the Atlantic Ocean. *Geochem. Techn. Rep.*, 8:803.
- Blow, W.H., 1969. Late Middle Eocene to Recent planktonic foraminiferal biostratigraphy. *Proc. 1st Int. Conf. Planktonic Microfossils, Geneva, 1967*: Leiden (E.J. Brill), 1:199–422.
- , 1979. *The Cainozoic Globigerinida*: Leiden (E.J. Brill).
- Bolli, H.M., and Saunders, J.B., 1985. Oligocene to Holocene low latitude planktic foraminifera. In Bolli, H.M., Saunders, J.B., and Perch-Nielsen, K. (Eds.), *Plankton Stratigraphy*: Cambridge (Cambridge Univ. Press), 155–262.
- Boltovskoy, E., 1976. Distribution of Recent foraminifera of the South American region. In Hedley, R.H., and Adams, C.G. (Eds.), *Foraminifera* (Vol. 2): London (Academic Press), 171–236.
- Boltovskoy, E., and Theyer, F., 1970. Foraminiferos Recientes de Chile Central. *Rev. Argentina Cienc. Nat. "Bernardina Rivadavia," Hidrobiol.*, 2:279–379.
- Boyce, R.E., 1976. Definitions and laboratory determination of compressional sound velocity parameters and wet-water content, wet-bulk density and porosity parameters by gravimetric and gamma-ray attenuation techniques. In Schlanger, S.O., Jackson, E.D., et al., *Init. Repts. DSDP*, 33: Washington (U.S. Govt. Printing Office), 931–958.
- Brady, H.B., 1884. Report on the Foraminifera dredged by H.M.S. *Challenger* during the years 1873–1876. *Rep. Sci. Results Challenger Exped., Zool.*, 9.
- Bullard, E.C., 1954. The flow of heat through the floor of the Atlantic Ocean. *Proc. R. Soc. London A*, 222:408–429.
- Caulte, J.-P., 1991. Radiolarians from the Kerguelen Plateau, Leg 119. In Barron, J., Larsen, B., et al., *Proc. ODP, Sci. Results*, 119: College Station, TX (Ocean Drilling Program), 513–546.
- Chen, P.-H., 1975. Antarctic radiolaria. In Hays, D.E., Frakes, L.A., et al., *Init. Repts. DSDP*, 28: Washington (U.S. Govt. Printing Office), 437–513.
- Curry, J.R., Moore, D.G., et al., 1982. *Init. Repts. DSDP*, 64, Pts. 1, 2: Washington (U.S. Govt. Printing Office).
- Davis, E., Mottl, M., Fisher, A., et al., in press. *Proc. ODP, Init. Repts.*, 139: College Station, TX (Ocean Drilling Program).
- Dewen, J.T., 1983. *Essentials of Modern Open Hole Log Interpretations*: Tulsa (Penwall).
- d'Orbigny, A., 1839. *Voyage dans l'Amerique Meridionale*. Foraminifères, 5.
- Fisher, A.T., and Hounslow, M., 1990. Heat flow through the toe of the Barbados accretionary complex. In Moore, J.C., Mascle, A., Taylor, E., et al., *Proc. ODP, Sci. Results*, 110: College Station, TX (Ocean Drilling Program), 345–363.
- Fisher, R.A., 1953. Dispersion on a sphere. *Proc. R. Soc. London A*, 217:295–305.
- Fisher, R.V., and Schmincke, H.-U., 1984. *Pyroclastic Rocks*: New York (Springer-Verlag).
- Gieskes, J.M., Gamo, T., and Brumsack, H., 1991. Chemical methods for interstitial water analysis aboard *JOIDES Resolution*. *ODP Tech. Note*, 15.
- Hays, J.D., 1965. Radiolaria and late Tertiary and Quaternary history of Antarctic seas. In Llano, G.A. (Ed.), *Biology of the Antarctic Seas II*. Am. Geophys. Union, Antarct. Res. Ser., 5:125–184.
- Hertzog, R., 1979. Laboratory and field evaluation of an inelastic-neutron-scattering and capture gamma-ray spectroscopy tool. *Soc. Pet. Eng. Pap.*, 7430.
- Horai, K., and Von Herzen, R.P., 1985. Measurement of heat flow on Leg 86 of the Deep Sea Drilling Project. In Heath, G.R., Burckle, L.H., et al., *Init. Repts. DSDP*, 86: Washington (U.S. Govt. Printing Office), 759–777.
- Hyndman, R.D., Langseth, M.G., and Von Herzen, R.P., 1987. Deep Sea Drilling Project geothermal measurements: a review. *Rev. Geophys.*, 25:1563–1582.
- Jaeger, J.C., 1961. The effect of the drilling fluid on temperatures measured in boreholes. *J. Geophys. Res.*, 66:563–569.
- Jenkins, D.G., 1985. Southern mid-latitude Paleocene to Holocene planktic foraminifera. In Bolli, H.M., Saunders, J.B., and Perch-Nielsen, K. (Eds.), *Plankton Stratigraphy*: Cambridge (Cambridge Univ. Press), 263–282.
- Kennett, J.P., and Srinivasan, M.S., 1983. *Neogene Planktonic Foraminifera*: Stroudsburg, PA (Hutchinson Ross).
- Kroenke, L.W., Berger, W.H., and Janecsek, T.R., et al., 1991. *Proc. ODP, Init. Repts.*, 130: College Station, TX (Ocean Drilling Program).
- Lambe, T.W., and Whitman, R.V., 1979. *Soil Mechanics* (SI edition): New York (Wiley).
- Lazarus, D., 1990. Middle Miocene to Recent radiolarians from the Weddell Sea, Leg 113. In Barker, P.F., Kennett, J.P. et al., *Proc. ODP, Sci. Results*, 11: College Station, TX (Ocean Drilling Program), 709–727.
- Lazarus, D., 1992. Antarctic Neogene radiolarians from the Kerguelen Plateau, Legs 119 and 120. In Wise, S.W., Jr., Schlich, R., et al., *Proc. ODP, Sci. Results*, 120: College Station, TX (Ocean Drilling Program), 785–809.
- Lundberg, N., and Moore, J.C., 1986. Macroscopic structural features in Deep Sea Drilling Project cores from forearc regions. *Mem.—Geol. Soc. Am.*, 166:13–44.
- Manheim, F.T., and Sayles, F.L., 1974. Composition and origin of interstitial waters of marine sediments based on deep sea drill cores. In Goldberg, E.D. (Ed.), *The Sea* (Vol. 5): New York (Wiley), 527–568.
- Martini, E., 1971. Standard Tertiary and Quaternary calcareous nannofossil zonation. In Farnacci, A. (Ed.), *Proc. 2nd Planktonic Conf. Roma*: Rome (Ed. Tecnosci.), 2:739–785.
- Martini, E., and Müller, C., 1986. Current Tertiary and Quaternary calcareous nannoplankton stratigraphy and correlations. *Newsl. Stratigr.*, 16:99–102.
- Matthews, D.J., 1939. *Tables of Velocity of Sound in Pore Water and in Seawater*: London (Admiralty, Hydrog. Dept.).
- Mazzullo, J.M., Meyer, A., and Kidd, R., 1987. New sediment classification scheme for the Ocean Drilling Program. In Mazzullo, J., and Graham, A.G., *Handbook for Shipboard Sedimentologists*. ODP Tech. Note, 8:45–67.
- Munsell Soil Color Charts, 1971. Baltimore (Munsell Color).
- Noorany, I., 1984. Phase relations in marine soils. *J. Geotech. Eng.*, 110:539–543.
- Norrish, K., and Hutton, J.T., 1969. An accurate X-ray spectrographic method for the analysis of a wide range of geological samples. *Geochim. Cosmochim. Acta*, 33:431–453.
- Ratcliffe, E.H., 1960. The thermal conductivities of ocean sediments. *J. Geophys. Res.*, 65:1535–1541.
- Resig, J.M., 1990. Benthic foraminiferal stratigraphy and paleoenvironments off Peru, Leg 112. In Suess, E., von Huene, R., et al., *Proc. ODP, Sci. Results*, 112: College Station, TX (Ocean Drilling Program), 263–296.
- Reynolds, R.C., 1967. Estimations of mass absorption coefficients by Compton scattering: improvements and extensions of the method. *Am. Mineral.*, 48:1133–1143.
- Sanfilippo, A., Westberg-Smith, M.J., and Riedel, W., 1985. Cenozoic radiolaria. In Bolli, H.M., Saunders, J.B., and Perch-Nielsen, K.

- (Eds.), *Plankton Stratigraphy*: Cambridge (Cambridge Univ. Press), 631–712.
- Schlumberger, 1989. *Log Interpretation Principles/Applications*: Houston (Schlumberger Educ. Services).
- Schrader, H.-J., and Gersonde, R., 1978. Diatoms and silicoflagellates. *Utrecht Micropaleontol. Bull.*, 17:129–176.
- Serra, O., 1984. *Fundamentals of Well Log Interpretation: Vol. 1. The Acquisition of Logging Data*: Amsterdam (Elsevier).
- _____, 1989. *Formation Microscanner Image Interpretation*: Houston (Schlumberger Educ. Services).
- Shepard, F., 1954. Nomenclature based on sand-silt-clay ratios. *J. Sediment. Petrol.*, 24:151–158.
- Shipboard Scientific Party, 1990. Explanatory Notes. In Rangin, C., Silver, E.A., von Breyman, M.T., et al., *Proc. ODP, Init. Repts.*, 124: College Station, TX (Ocean Drilling Program), 17–33.
- Srinivasan, M.S., and Kennett, J.P., 1981. A review of Neogene planktonic foraminiferal biostratigraphy: applications in the Equatorial and South Pacific. *Spec. Publ.—Soc. Econ. Paleontol. Mineral.*, 32:395–432.
- Taira, A., Hill, I., Firth, J.V., et al., 1991. *Proc ODP, Init. Repts.*, 131: College Station, TX (Ocean Drilling Program).
- Timur, A., and Toksoz, M.N., 1985. Fundamentals of well log interpretation. *Ann. Rev. Earth Planet. Sci.*, 13:315–344.
- Vacquier, V., 1985. The measurement of thermal conductivity of solids with a transient linear heat source on the plane surface of a poorly conducting body. *Earth Planet. Sci. Lett.*, 74:275–279.
- van Morkhoven, F.P.C.M., Berggren, W.A., and Edwards, A.S., 1986. Cenozoic cosmopolitan deep-water benthic foraminifera. *Bull. Cent. Rech. Explor.-Prod. Elf-Aquitaine, Mem.*, 11:1–421.
- Von Herzen, R.P., and Maxwell, A.E., 1959. The measurements of thermal conductivity of deep-sea sediments by a needle probe method. *J. Geophys. Res.*, 64:1557–1563.
- Wentworth, C.K., 1922. A scale of grade and class terms for clastic sediments. *J. Geol.*, 30:377–392.
- Yokota, T., Kinoshita, H., and Uyeda, S., 1980. New DSDP (Deep Sea Drilling Project) downhole temperature probe utilizing IC RAM (memory) elements. *Tokyo Daigaku Jishin Kenkyusho*, 55:75–88.
- Zijderveld, J.D.A., 1967. A.C. demagnetization of rocks: analysis of results. In Collinson, D.W., Creer, K.M., and Runcorn, S.K. (Eds.), *Methods in Palaeomagnetism*: Amsterdam (Elsevier), 368–371.

Ms 141IR-105